



Sedimentary facies analysis of the Mesozoic clastic rocks in Southern Peru (Tacna, 18°S): Towards a paleoenvironmental Redefinition and stratigraphic Reorganization



Aldo Alván^{a,*}, Javier Jacay^b, Luca Caracciolo^c, Elvis Sánchez^a, Inés Trinidad^a

^a Instituto Geológico Minero y Metalúrgico (INGEMMET), Dirección de Geología Regional, Av. Canadá 1470, San Borja, Lima 41, Peru

^b Universidad Nacional Mayor de San Marcos, Escuela de Ingeniería Geológica, Av. Venezuela Cdr. 34, Lima, Peru

^c Friedrich-Alexander Erlangen University (FAU) Erlangen-Nuremberg, GeoZentrum Nordbayern, Schlossgarten 5, 91054, Erlangen, Germany

ARTICLE INFO

Keywords:

Yura Group
Hualhuani Formation
Mesozoic Arequipa Basin
Central Andes
Facies Analysis

ABSTRACT

The Mesozoic rocks of southern Peru comprise a Middle Jurassic to Early Cretaceous sedimentary sequence deposited during a time interval of approximately 34 Myr. In Tacna, these rocks are detrital and constitute the Yura Group (Callovian to Tithonian) and the Hualhuani Formation (Berriasian). Basing on robust interpretation of facies and petrographic analysis, we reconstruct the depositional settings of such units and provide a refined stratigraphic framework. Accordingly, nine types of sedimentary facies and six architectural elements are defined. They preserve the record of a progradational fluvial system, in which two styles regulated the dispersion of sediments: (i) a high-to moderate-sinuosity meandering setting (Yura Group), and a later (ii) incipient braided setting (Hualhuani Formation).

The Yura Group (Callovian-Tithonian) represents the onset of floodplain deposits and lateral accretion of point-bar deposits sited on a semi-flat topography. Nonetheless, the progradational sequence was affected by at least two rapid marine incursions occurred during Middle Callovian and Tithonian times. Such marine incursions reveal the proximity of a shallow marine setting and incipient carbonate deposition. In response to increase in topographic gradient, the Hualhuani Formation (Berriasian) deposited as extensive multistory sandy channels. The mineralogy of the Mesozoic sediments suggests sediment supplies and intense recycling from a craton interior (i.e. Amazon Craton and/or plutonic sources) located eastward of the study area.

1. Introduction

The Arequipa-Tarapacá Basin has been an extensive depression stretching along the western margin of South America, between southern Peru and northern Chile (Vicente, 1981). To the west, the basin was bordered by andesitic rocks of both the Chocolate (in southern Peru, Vicente, 2005) and La Negra (in northern Chile, Oliveros et al., 2006) Formations. The eastern border remains unknown; however, there are numerous studies affirming that such border was located in Puno (70°W) along the Cuzco-Lagunillas-Mañazo Faults System (e.g. Carlotto et al., 2009; Alván, 2009). Besides the uncertainty of the paleobasin borders, the internal chronostratigraphic definition and boundaries are also matter of numerous studies and debates since the 50's decade, and will remain in discussions while there is no consistent paleogeographic overview of the basin.

A high-resolution analysis of the Mesozoic sedimentary facies of southernmost Peru (Tacna, 18°S) and a review of their mineral

composition is necessary to define a consistent paleogeographic model. The aim is to provide the best arguments for a paleoenvironmental characterization, which in turn can be used to propose a coherent stratigraphic reorganization. The facies analysis is carried out by using the classification codes of Miall (1985, 1996) for fluvial deposits. The mineral composition is defined for the first time following the method of Gazzi-Dickinson to provide insights into their provenance and to better understand their depositional history. The integration of facies analysis and petrographic data can provide a more comprehensive picture of the both provenance and tectonic setting. Furthermore, the definition of systems tracts (compared to the global sea-level fluctuations schemes of both Haq et al., 1987 and Hardenbol et al., 1998) in light of major tectonic events will provide key elements for reconstructing the Jurassic to Early Cretaceous geodynamic evolution of the Province of Tacna. Overall, we present consistent arguments to re-evaluate the basin fill by a new mapping, facies analysis (Section 4) and petrography of sandstones (Section 5). Finally, we re-organize the

* Corresponding author.

E-mail address: aalvan@ingemmet.gob.pe (A. Alván).



Fig. 1. Location of the main Mesozoic sedimentary basins in South America (selected in light blue). The extensions and boundaries are inferred from von Hillebrandt (1987), Jaillard and Jacay (1989), Jaillard et al. (1990, 2000), Parent (2006) and Alván (2009). Red chart indicates southern Peruvian localities involved in this study. (For interpretation of the references to colour in this figure legend, the reader is referred to the web version of this article.)

Mesozoic stratigraphy of southern Peru.

2. Geological setting

The Late Paleozoic – Late Triassic break-up and fragmentation of Pangea was followed by the Gondwana Orogeny of the Central and Southern Andes (Jaillard et al., 2000) and rifting-extensional processes on the western margin of South America (cf. Ramos, 2009; Ramos and Aleman, 2000). According to these authors, the most relevant consequences following the fragmentation is the formation of syn-rift oceans along the western margin of Gondwana, where extensional (or transtensional) processes continued until Early Jurassic time. Such processes triggered the formation of the back-arc Arequipa-Tarapacá Basin (Sempere et al., 2002; Vicente, 2006) (Fig. 1) and consequent accumulation of syn-rift deposits.

The initial filling of the Arequipa-Tarapacá Basin consists of thick piles (> 2000 m) of Late Triassic to Early Jurassic primary volcanic rocks (andesites and basalts, cf. Jenks, 1945; Boekhout et al., 2013), attributed to volcanic products of the Chocolate Volcanic Arc (Mamani et al., 2010) (Fig. 2). These volcanic rocks extend from Ica (14°S) to Arequipa (16°S) and Tacna (18°S) and are grouped within the “Chocolate Formation” (Jenks, 1945) and “Junerata Formation” (Wilson and García, 1962). Similar rocks are documented farther south in northern Chile (18°–36°S) where they are known as the La Negra Formation (von Hillebrandt and Schmidt-Effing, 1981; Bell and Suarez, 1995; Oliveros et al., 2006) (right side of the Fig. 2). According to Martínez et al. (2012) and Oliveros et al. (2012), half-grabens facilitated most of the Mesozoic volcanism in that region.

The deposition of extensive carbonate platforms (mudstones, wackestones, grainstones and claystones) initiated since late Early Jurassic and protracted until the early Middle Jurassic with the deposition of the Pelado and Socosani formations (Wilson and García, 1962; Monge and Cervantes, 2000). These units occur in Arequipa and consist of a ca. 80 m thick pile of sediments (Jenks, 1945), while in Tacna the thickness of comparable stratigraphic levels is of ca. 200 m (Wilson and García, 1962). Between the late Middle Jurassic and Early Cretaceous time, clastic sedimentation took place extensively in

southern Peru, forming the Yura Group (Jenks, 1945; Benavides, 1962; Vargas, 1970; Vicente, 1981) (see Section 3 for further details). According to Sempere et al. (2002), Martínez and Cervantes (2003) and Mamani et al. (2010), the syn-rift Middle Jurassic volcanism (i.e. Guaneros Formation) developed synchronous to clastic sedimentation in some areas of southern Peru (e.g. Moquegua, 17°S).

3. Stratigraphy of the Mesozoic Arequipa-Tarapacá Basin-fill and the inconsistencies of along the provinces of Arequipa (16°S) and Tacna (18°S)

Exposures of Mesozoic detrital rocks cover a wide area in southern Peru, including the provinces of Ayacucho (14°S), Huancavelica (15°S), Arequipa (16°S), Moquegua (17°S) and Tacna (18°S) (Palacios, 1995). Nonetheless, these strata are discontinuous and occur as patchy remnants. Jenks (1945) and Benavides (1962) were the firsts studying these rocks in the province of Arequipa, naming them as “Yura Group” and assigning a depositional age of Middle Jurassic to Early Cretaceous. According to Benavides (1962), the stratotype of the Yura Group (Arequipa) sums up to 2152 m in thickness and is divided into 5 members (or lithostratigraphic units) namely Puente, Cachíos, Labra, Gramadal and Hualhuani (see details in Fig. 2). Following the descriptions of Benavides (1962), the Puente Formation (600 m thick) consists of arkoses and quartzose sandstones, often interbedded by black claystones. Up section, the Cachíos Formation consists of black claystones often including layers of quartzose sandstone (603 m thick). The overlying Labra Formation is composed of quartzose sandstones and interbedded black claystones (807 m thick). Upward, the Gramadal Formation consists of grey limestones and subordinate claystones (82 m thick). A gentle unconformity marks the boundary with the overlying Hualhuani Formation which consists of cross-stratified quartzose sandstones (60 m thick). About 200 km farther south (Tacna), Wilson and García (1962) described a similar terrigenous pile of ca. 1606 m thick, which they attributed to the Yura Group. Although these authors used the stratigraphic nomenclature of Arequipa, its internal stratigraphic configuration was divided into two members only i.e. the Ataspaca Formation (ca. 1093 m) and Chachacumane Formation (ca.

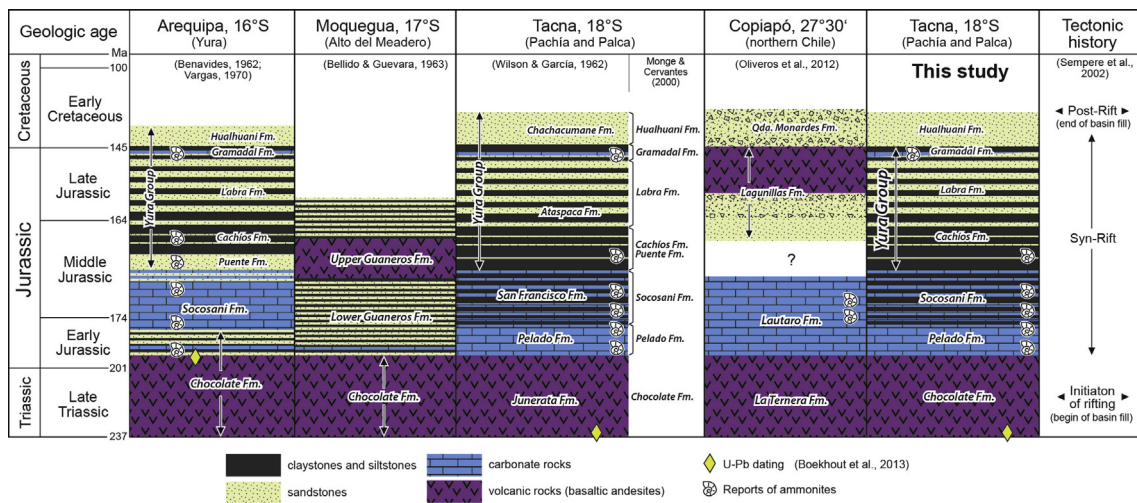


Fig. 2. Comparison of stratigraphy along Mesozoic outcrops between Arequipa (southern Peru) and Copiapó (northern Chile). The stratigraphy of the Arequipa Basin-fill is taken from Benavides (1962) and Vicente (1989), of Moquegua after Bellido and Guevara (1963), of Tacna after Wilson and García (1962) and Monge and Cervantes (2000), and of Copiapó by Oliveros et al. (2012). The U-Pb dating was taken from Boekhout et al. (2012; 2013), and ammonite reports by Wilson and García (1962), Benavides (1962), Westermann et al. (1980), Vicente (1981), von Hillebrandt and Schmidt-Effing (1981), von Hillebrandt (1987), Alván et al. (2010), INGEMMET (2016) and Benites (2017). The tectonic history is based on Sempere et al. (2002).

513 m) (Fig. 2). In such context, we also highlight a notorious difference in lithology and an unconformity between such deposits, which have implications on the stratigraphic framework of southern Peru.

The current Mesozoic stratigraphic subdivision in Tacna refers to the works of Vicente (1981), Vicente et al. (1982), Monge and Cervantes (2000) and Acosta et al. (2011) in which the Yura Group comprises a 34 Myr sequence and includes the Puente, Cachíos, Labra, Gramadal and Hualhuani Formations (similar to Arequipa). Nonetheless, this study demonstrates that some of these units are not present in Tacna. Vicente (1981) and Vicente et al. (1982) suggested a deep-marine setting as main depositional environment for most of the Mesozoic sediments, and provided a provenance framework suggesting arrivals from the Chocolate Volcanic Arc. However, the numerous evidences of a rift system and fluvial influence challenge this statement.

4. Facies analysis of the Arequipa Basin-fill in Tacna

Since the Early Cenozoic, the Andean Orogeny caused intense tectonic deformation that triggered to continuous uplift and erosion of older sedimentary rocks in the region (cf. Oncken et al., 2006). Consequently, good-quality outcrops are rare and dislocated along major valleys of the main rivers of southern Peru (e.g. the Vitor River in Arequipa (16°S) and the Palca River in Tacna (18°S)). The best exposures in the Province of Tacna are located in Ataspaca, Copapuquio and Tocuco, allowing a refined geological mapping (Figs. 3 and 4), the definition of nine sedimentary facies (Fig. 5) and the measurement of four vertical stratigraphic logs (Fig. 6) at Quebrada Chachacumane (Fig. 6A), Quebrada Ataspaca (Fig. 6B), Quebrada Tocuco (Fig. 6C) and Cerro Challatita (Fig. 6D). The analysis of the sedimentary facies has been carried out by using the codes proposed by Miall (1996) to describe ancient fluvial sediments. The Yura Group of Wilson and García (1962) can be divided into two main parts according to a facies association, (i) fine-grained sediments i.e. dark grey/black claystones and siltstones (most of which are abundant in the lower Yura Group), and (ii) quartzose sandstones.

According to the facies classification shown in Fig. 5, sandstones are grouped into facies “Sx” (Cross bedded sandstone), “Sh” (Planar bedded sandstone with parallel laminations), “Sm” (Massive sandstone), and facies “Sr” (Ripple cross laminated sandstone). Pelitic sediments are classified as facies “Fm” (Massive black claystone and siltstone), “Fl” (Laminated and tabular black claystones and siltstones), and “Ff” (Black

claystones and siltstones with flaser bedding and slumps). Finally, carbonate facies are classified into “Fca” (Coarse-grained carbonate sediments) and “Cca” (Fine-grained carbonate sediments).

4.1. Cross bedded sandstones (Sx)

The Sx facies consists of light-grey to grey whitish coarse-to fine-grained quartzarenites with cross-stratified structures. Sandstones of the facies Sx are predominantly composed of sub-rounded to sub-angular monocrystalline (Qm) and undulate quartz grains (Qo). Sandstones of this lithofacies are organized in tabular strata usually tilted in ca. 15° (or irregular) and are internally composed of inclined layers i.e. (trough) cross-bedding structures (Fig. 7A). The base of the stratum is generally erosive and is made of coarse-grained sediments. Scours and fill in the angle-varying base are common features. Some of the thin laminae include dark grey sediments within the cross lamination and often as sags along this facies. Commonly facies Sx alternates with strata containing ripple marks (facies Sr) (Fig. 8C). When cross laminations are low angled, they are consistent with the direction of the paleocurrents measured from ripple marks. The upper contact of this facies generally grades into finer facies (i.e. facies Fl) and more rarely into facies Fm (Fig. 8A) or into facies Sh (Fig. 7E). Sx sandstones occur predominantly in the uppermost part of the Quebrada Chachacumane, Quebrada Ataspaca, Quebrada Tocuco and Cerro Challatita sections, while it occurs in much lower amounts along the lowermost part of the Quebrada Chachacumane, Quebrada Ataspaca and Cerro Challatita sections. Small amounts of bitumen are found within the pore space.

4.2. Planar bedded sandstone with parallel lamination (Sh)

The Sh facies consists of medium-to fine-grained (quartzose) sandstones. Grains are well to moderately sorted, and are commonly arranged in parallel stratification and lamination (Fig. 7B). Nonetheless, the Sh sandstones are often massive or structureless. Sandstones of this lithofacies are arranged in strata less than 1 m thick displaying tabular geometry (Fig. 9D), and are usually associated with facies Sx (interbedding). Sh sandstones commonly contain trace fossils (burrows) of horizontal trajectory (Fig. 8D). Strata of this facies rarely alternate with tabular strata with no internal structures (facies Sm) and with sediments of facies Fl and/or Fm. The facies Sh occur in the Cerro Chachacumane and Quebrada Ataspaca sections, and in the uppermost parts of the

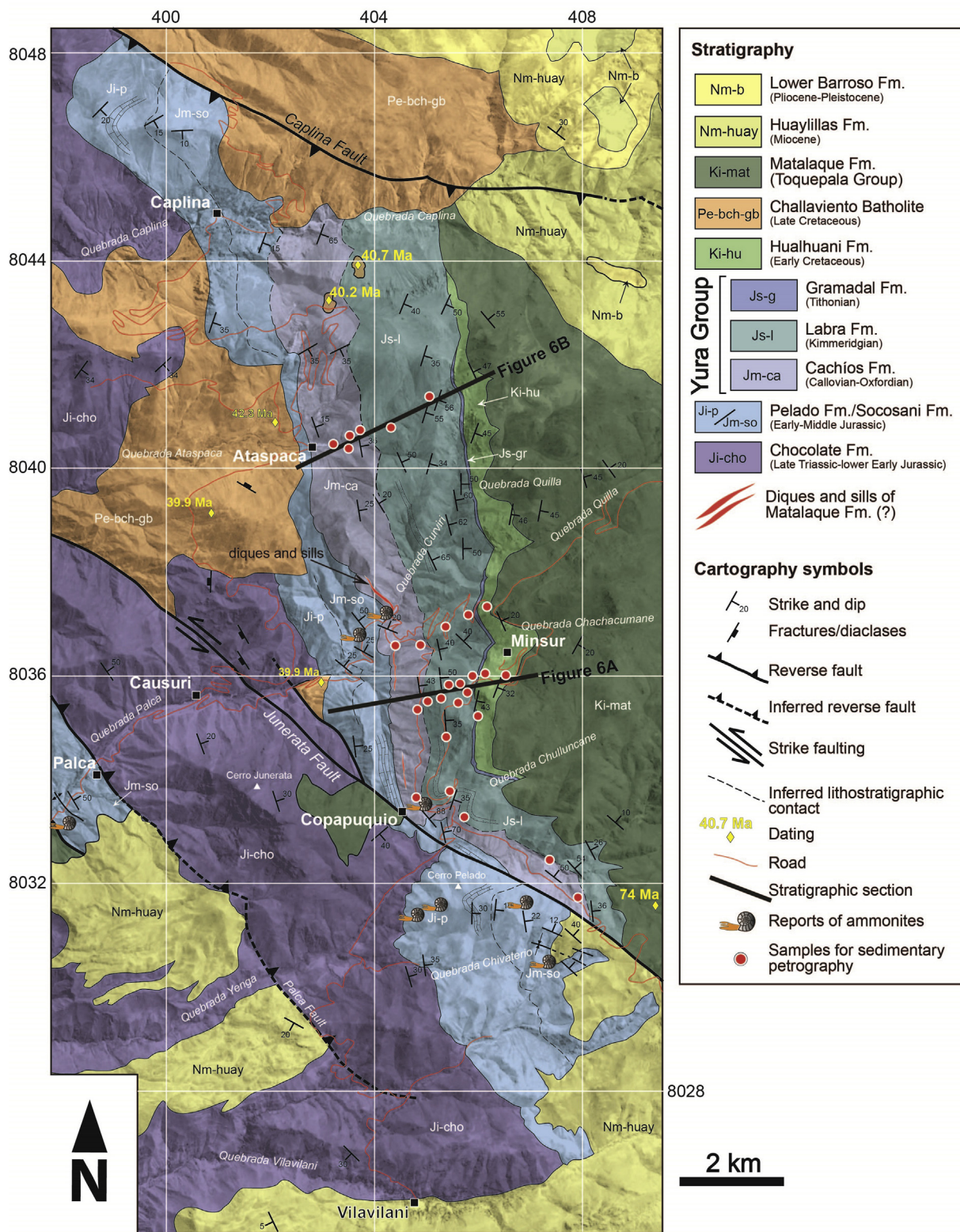


Fig. 3. Local geological map of Ataspaca, Palca and Copapuquio, west of Tacna (INGEMMET, 2016), after Monge and Cervantes (2000) and Acosta et al. (2011). A refined stratigraphic framework is proposed in this study. The stratigraphic sections are indicated in black thick lines and refer to the Figs. 6A and 6B. To see details on the sampling refer to Fig. 11. Radiometric ages (yellow numbers) are provided in Clark et al. (1990) and Martínez and Cervantes (2003). (For interpretation of the references to colour in this figure legend, the reader is referred to the web version of this article.)

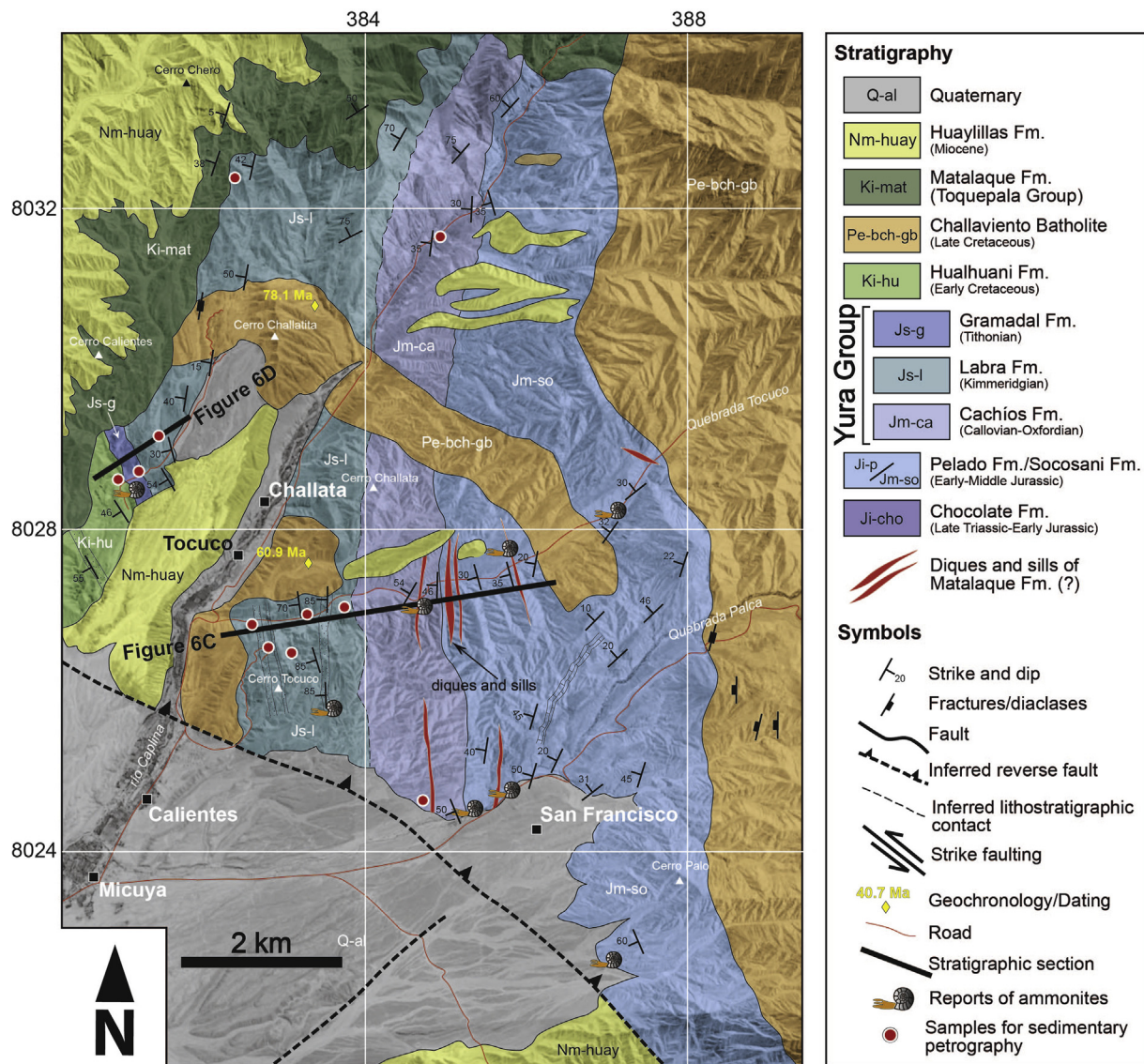


Fig. 4. Local geological map of Tocado, east of Tacna, after Monge and Cervantes (2000), Acosta et al. (2011) and INGEMMET (2016). A refined stratigraphic framework is proposed in this study. The stratigraphic sections are indicated in black lines, and refers to Figs. 6C and 6D. Radiometric ages (yellow numbers) are provided in Clark et al. (1990). (For interpretation of the references to colour in this figure legend, the reader is referred to the web version of this article.)

Quebrada Tocado and Cerro Challatita logs.

4.3. Massive sandstone (Sm)

The *Sm* facies consists of massive coarse-to fine-grained quartzarenites with features consisting of moderately sorted sub-rounded to sub-angular grains. This lithofacies commonly appears in strata thicker than 1 m without internal structures. Nonetheless, rarely is possible to observe very poor parallel lamination. Sediments of this facies commonly alternate with tabular strata with low angled (< 20°) parallel lamination (*Sh* facies) and with cross-bedded sandstones (*Sx* facies), as shown in Fig. 8B and C. Paleocurrents measured on cross laminations are multidirectional, and are consistent with the direction measured in some of the ripple marks of facies *Sr*. Small proportions of bitumen commonly occur within pores. The *Sm* facies is observed along the Quebrada Chachacumane, Quebrada Ataspaca, Quebrada Tocado and Cerro Challatita sections.

4.4. Ripple cross laminated sandstone (Sr)

Sandstones belonging to facies *Sr* are mostly medium-to fine-grained quartzarenites and subarkoses. These are moderately well sorted and consist of sub-rounded monocrystalline quartz grains. Sedimentary structures are mostly asymmetrical ripple marks commonly in bedding of 50 cm to 1 m thick (Fig. 7C and D). Dark grey minerals organized in thin laminae within ripples are common. Facies *Sr* alternate with strata containing cross laminations (facies *Sx*) and planar bedding/laminations (facies *Sh*). The *Sr* lithofacies facies is commonly overlaid or capped by massive or laminated claystones and/or siltstones (facies *Fm* and/or *Fl*, see Sections 3.5 and 3.6). The *Sr* facies is observed in the uppermost part of the Quebrada Chachacumane, the Quebrada Ataspaca and Cerro Challatita sections.

4.5. Massive black claystone and siltstone (Fm)

Sediments of the *Fm* facies consist of mostly dark grey/black claystones and siltstones. These sediments are arranged into massive strata displaying tabular geometry of approximately 3 m thick (Fig. 8A).

Facies types (FT)	Lithology, sedimentary structures and thicknesses	Key Face	Trend	Depositional context	Occurrence
Sx	Coarse- to fine-grained sandstones, with cross (often trough) lamination ($\pm 15^\circ$) and straight stratification, commonly with erosive base. Often scour and fill deposits are observed with variable angle base.		Shallowing	Lower flow regime, usually with crevasse splays and often antidunes. Transverse bars are common.	In upper and lower part of Hualhuani Fm., in middle Labra Fm. and in the upper Cachíos Fm.
Sh	Medium- to fine-grained sandstones, with horizontal and parallel stratification/lamination, generally in tabular arrangement (<1 m thick). Often structureless (massive). Trace fossils (burrows) are common, and are parallel to the stratification.			Planar bed flow, more possibly upper flow regime than lower. Lateral and rapid deposition in wide platforms with uniform regime. Absence of channels.	Labra Fm., and the lower part of the Gramadal Fm.
Sm	Coarse- to fine-grained sandstones, in massive (structureless) strata. Facies Sm appears at least more than 1 m thick. Sometimes very poor lamination.			Lateral persistent deposition in wide platforms with uniform and constant regime, no channels.	Cachíos Fm. Labra Fm. and lower Hualhuani Fm.
Sr	Medium- to fine-grained sandstones containing dominantly ripples marks, commonly unidirectional. Strata with facies Sr often shows between 0.5 and 1 m thickness. Often appears horizontal burrows.			Ripples typical of lower flow regime, and near to a beach.	Labra Fm., Cachíos Fm. and the lower part of the Hualhuani Fm.
Fm	Claystones to siltstones commonly massive and black, often dark grey. Often these sediments are carbonaceous (especially if they appear in Puente/ Cachíos Fm.). Strata with Fm commonly show 2 m thick, and 5 m thick maximum. Rarely it is 20 cm thick.			Overbank and waning flood deposits in floodplain, with low settlement.	Cachíos Fm. and in lower Labra Fm.
Fl	Claystones and siltstones typically black, commonly with parallel lamination. Facies Fl appears commonly in strata up to 0.50 m thick or less. Commonly mudcracks, bioturbation (ichnofacies) and fragments of fossil plants are observed.			Overbank and waning flood deposits in floodplain, rapid settlement in drape deposits. Backswamps.	Labra Fm. and Gramadal Fm.
Ff	Alternated claystones and siltstones featured by flaser/lenticular bedding, often with parallel lamination (weak), and convolute laminations (slumps). Claystones are typically black to dark grey colour. Bedding up to 0.5 m thick.			Bidirectional currents in backswamp deposits where the floodplain is, behind levees. Intertidal environments, and/or point-bars in ephemeral streams.	Lower and middle part of the Cachíos Fm. Rarely in the Gramadal Fm.
Cca	Alternating carbonaceous siltstones/sandstones and coarse-grained limestones (i.e. rudstones, floatstones and grainstones, often with fossil brachiopods, bivalves and ammonites).			Platforms with organic accumulations and/or swamps. Internal platform or barrier.	Gramadal Fm. (of Cerro Challatita).
Fca	Carbonaceous claystones and siltstones alternating with fine-grained sandstones. Often with mud films and mudcracks. Usually appears thin layers of fine-grained limestones, but not continuous laterally.			Platforms with organic accumulations and/or swamps. Protected platform.	Gramadal Fm. (of Quebrada Chachacumane).

Sedimentary structures

- Flaser bedding
- Ripples
- Fossil plants
- Parallel lamination
- Slumps
- Mudcracks

Fossils

- Fragments of mollusks
- Ammonites
- Burrows

Fig. 5. Summary of characteristic facies types on the Mesozoic sedimentary rocks of Tacna, and their respective depositional context.

Thinner layers (0.5 m thick) of the *Fm* facies are observed in Quebrada Chachacumane and Quebrada Tocuco sections (Fig. 8C). The *Fm* facies extends laterally for about 7 km length. Claystones and siltstones occur as thin beds or lenticular forms of up to 0.5 m thick (when they are associated with sandy facies). Furthermore, it is possible to observe some lenticular or sheet-like horizons of less than 0.5 m thick containing some fossil plants and small concretions of < 1 cm in diameter. The *Fm* facies is often interlayered with very fine-grained ammonite-rich (Callovian) calcareous sandstones/siltstones (*Fca* facies, see Section 4.9 for further details) and are particularly concentrated in the basal strata of the Cachíos Formation (e.g. the Quebrada Tocuco, Quebrada Ataspaca and Quebrada Chachacumane logs). Sediments of the *Fm* facies are mostly found in the topmost part of a fining-upward sequence, commonly starting with *Sx*, *Sr* and/or *Sh* sandstones (see Fig. 8D and C). The *Fm* facies occur predominantly in the lowermost part of the Yura Group, along the Quebrada Ataspaca, Quebrada Chachacumane and Quebrada Tocuco sections.

4.6. Laminated and tabular black claystone and siltstone (*Fl*)

The *Fl* facies consists of black to dark grey claystones and siltstones that are geometrically arranged in thin beds of maximum 50 cm thickness. The strata containing this lithofacies are laterally very extensive and exhibit sheet-like geometry (Fig. 9A). The *Fl* facies includes millimetre-thick laminations composed of white greyish very fine-grained sandstone laminae. Mudcracks are common and their fissures are filled with grey siltstones or very fine-grained sandstones. Sediments from this facies are also associated with large-scale boudinages (Fig. 9A) and contain fragments of fossil plants and bioturbation (burrows) of vertical traces slightly perpendicular to stratification. Small iron concretions are also frequently observed. Strata of this facies

appear gradationally above sandstones of the facies *Sh*, *Sr* and rarely *Sx* facies. Remarkably, most of claystones and siltstones are deformed by centimetre-scale synsedimentary normal faults. Fine-grained sediments of the *Fl* facies are predominantly observed in the lowermost part of the Quebrada Chachacumane and Quebrada Ataspaca sections, and in lower proportion in the lowermost part of the Quebrada Tocuco and Cerro Challatita sections.

4.7. Black claystone and siltstone with lenticular/flaser bedding and slumps (*Ff*)

Sediments of the *Ff* facies are very similar to those of the *Fl* facies, although differences exist. The *Ff* facies consist of alternating claystones and siltstones of dark grey to black colour, rarely with fragments of plant fossils. The internal organization reflects a dominance of asymmetrical structures like lenticular and flaser bedding (or simply wavy bedding), which are geometrically structured in laterally extensive (similar to facies *Fl*) tabular bodies of up to 50 cm thick (Fig. 9C). Paleocurrent directions measured on lenticular structures are generally polymodal, although dominant NW and SW directions prevail. Paleocurrent data for this facies are consistent with equivalent data obtained from ripples and cross laminations of adjacent strata (facies *Sx* and *Sr*). The *Ff* facies is locally observed along the lower part of the Quebrada Ataspaca section (e.g. within the lower part of the Cachíos Formation and within the Gramadal Formation).

The *Ff* facies can include deformation features as convolute laminae (Fig. 9B). Such sediments are commonly observed in the lower part of the Quebrada Chachacumane and Quebrada Ataspaca sections (i.e. lower part of the Cachíos Formation), and more frequently in the middle part of the Quebrada Tocuco section. The *Ff* facies is used in this study as a valuable tool for stratigraphic correlations (see further details

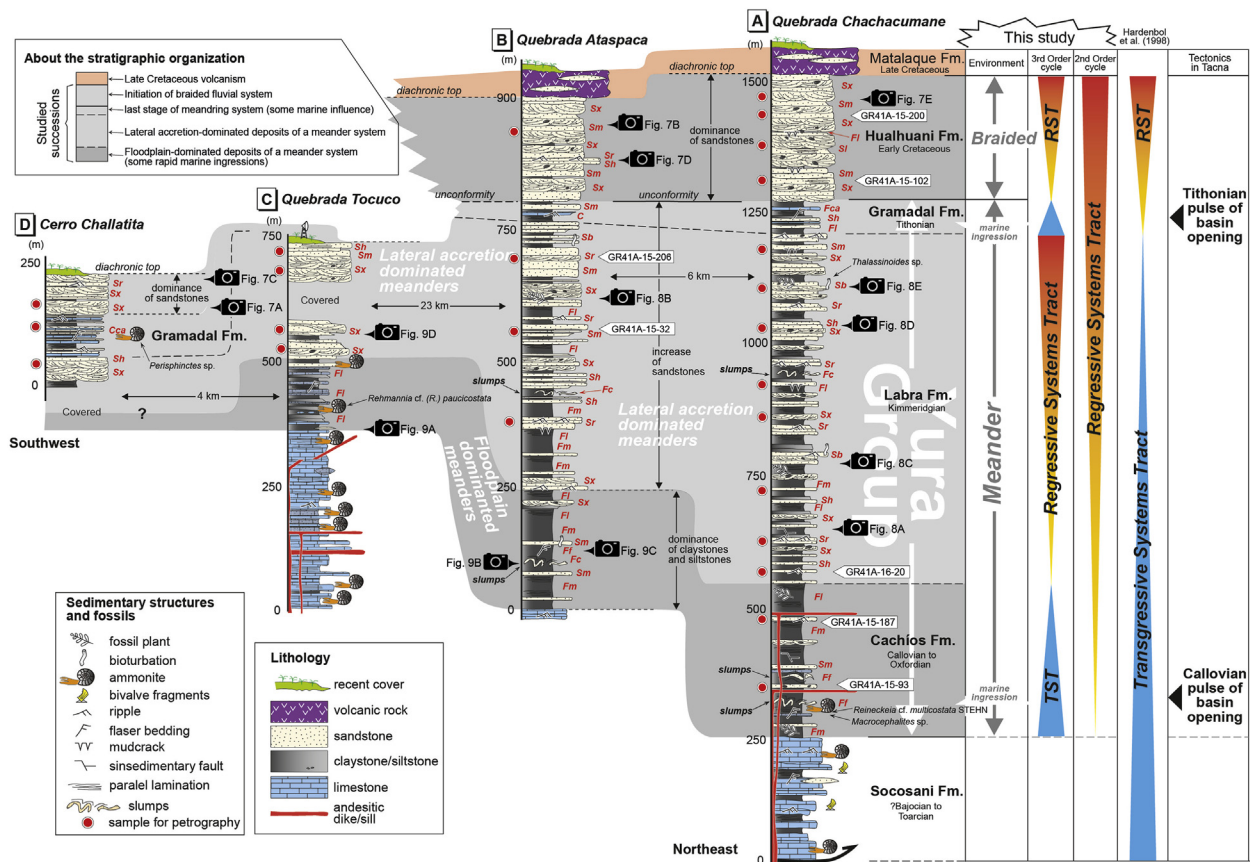


Fig. 6. Stratigraphic sections measured in Tacna, i.e. Quebrada Chachacumane (± 6 km northeast of Palca), Quebrada Ataspaca (next to the town of Ataspaca), Quebrada Tocuco (± 7 km northeast of Pachía), and Challatita (± 3 km northwest the town of Calientes). A refined stratigraphic reorganization is proposed in this figure. Red cursive letters indicate codes for sedimentary facies detailed in Fig. 5. Reference of Callovian and Tithonian ammonites are taken from Westermann et al. (1980), Alván et al. (2010) and INGEMMET (2016). A third order cycle represents events of less than 3 Myr, while a second order cycle represents events between 3 and 50 Myr (after Schumm, 1981 and Vail et al., 1991). For a better overview of the sample position refer to the Fig. 11. The two pulses of subsidence are discussed in the Section 8.3. Abbreviations: TST = transgressive systems tract, RST = regressive systems tract. (For interpretation of the references to colour in this figure legend, the reader is referred to the web version of this article.)

in Section 7.1).

4.8. Mixed coarse-grained carbonate-siliciclastic sediments (Cca)

The Cca facies consists of coarse-grained limestones, which is commonly associated to quartzose sandstones (facies Sx and Sr), fine-grained sediments (Fl facies) and often fine-grained calcareous sediments (Fca facies). Carbonate-rich siltstones and claystones usually have a dark grey colour. According to the petrographic classification of Dunham (1962) and Embry and Klován (1971), limestones are commonly rudstones and floatstones with grainstones and wackestones matrix. They generally include molluscs and bivalves, and often ammonites (Tithonian). Strata with this facies are only observed along the exposures of the Cerro Challatita section.

4.9. Mixed fine-grained carbonated-siliciclastic sediments (Fca)

Sediments of the Fca facies are composed of very fine-grained carbonate detritus alternating with fine-grained limestone. According to the classification of Dunham (1962), such rocks are mudstones and wackestones. The very fine-grained sediments consist of dark grey carbonated siltstones and claystones (marls). Mudcracks are common within this lithofacies. The Fca and Cca lithofacies are the only having carbonate components. However, facies Fca and Cca differ from the Fm facies because of the presence of interlayered limestone. The facies Fm is massive and include fine-grained detrital components but doesn't

include any limestone s.s. (e.g. mudstones and wackestones). Carbonate-rich sediments of the Fca facies concentrate in the middle outcrops of the lower and middle part of the Quebrada Chachacumane section (see more detail in Section 5.6), and frequently include ammonites of Callovian age, when these are associated to slumps and flaser/lenticular bedding.

5. Facies associations and architectural elements of the Arequipa Basin-fill in Tacna

Basing on Miall (1985), six architectural elements are identified in the Mesozoic Arequipa Basin in Tacna according to their internal lithofacies (i.e. structures, lithology, fossils, depositional geometry, as well as paleocurrent indicators and lateral/vertical arrangement of the lithofacies) (Fig. 10). The defined architectural elements are (i) Channels (CH), (ii) Sandy bedforms (SB), (iii) Lateral accretion (LA), (iv) Laminated sand sheets (LS), (v) Floodplains (FF), and (vi) Shallow lake deposits (SL). Fig. 11 shows a schematic overview of the distribution of most of the elements defined in this study.

5.1. Channel-fill elements (CH)

5.1.1. Description

The CH architectural element is made of up to 10 m thick coarse-grained sand bodies. Strata of this element show gently inclined tabular geometry often occurring as large-scale lenticular geometry. The

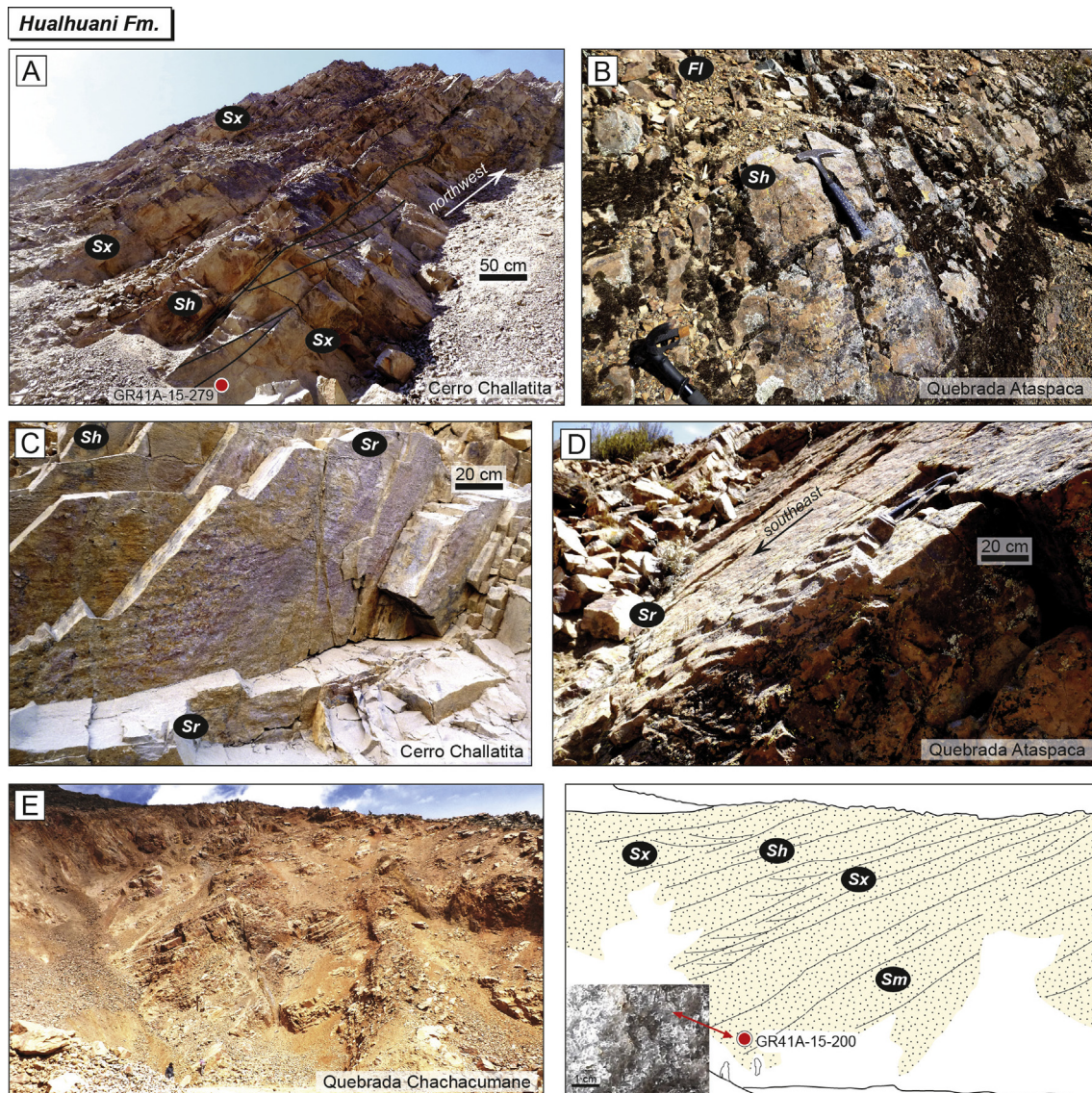


Fig. 7. Outcrops of the Hualhuani Formation in Tacna. In A: Cross-stratified and laminated sandstones (facies *Sx* and *Sh*). In B: Fining-upward sequence of massive sandstones to siltstones (facies *Sm* and *Fl*). In C and D: Sandstones of the *Sr* facies, showing unidirectional ripple marks. In E: Massive and cross-stratified quartzose sandstones (zoom). See the stratigraphic position of photos in the Fig. 6.

channel character consists of sedimentary bodies pinching-out laterally and corresponding to the flanks of a channel. The typical lithofacies of the element *CH* are *Sx*, *Sm*, *Sr* and *Sh*. Erosional basal surfaces (although weak or low-angled) are observed locally, and commonly show an irregular contact, with up to 0.5 m of assumed incised relief. Its upper surface shows vertical gradations, changing from coarse-grained sandstones to finer sequences, commonly alternating between facies *Sr* and *Sh*. This gradation marks the beginning of each of the fining-upward sequence. In most cases these sequences are topped by either massive facies (*Fm*) or thin strata of black claystones and siltstones (facies *Fl*). When no claystones or siltstones occur (i.e. *Fl* and/or *Fm* facies), these deposits reflect total sandy accumulations (as observed in along the Hualhuani Formation), and are easily to follow during field observation (e.g. along Cerro Chachacumane, Figs. 3 and 11).

5.1.2. Interpretation

The presence of *CH* elements is commonly attributed to the effect of sediment-fill vertical stacking of major channel belts, as suggested by the presence of basal erosive surfaces (although gentle and low angled) in relation to the underlying deposits. The latter can also occur in

deposits of other architectural elements (for instance, elements *LA*, *SB* and *LS*). It is common to observe an association among the elements *CH* and *FF* within the Labra Formation. Conversely, such association is rare in the uppermost strata of the Mesozoic pile (Hualhuani Formation). All these features indicate that the formation of channels developed as a consequence of the avulsion of river channels during sandy body's migration (e.g. Smith et al., 1989) and leads deposition of downward (as well as lateral) accumulation of sediments as multistory sandy deposits (cf. Miall, 2014). The element *CH* is intimately related to the element *LA* (see Section 5.2) and often to the element *SB*.

5.2. Lateral accretion elements (LA)

5.2.1. Description

The *LA* element is the most abundant deposit found in the Mesozoic sediments of Tacna. The *LA* element is commonly exposed as large-scale and lenticular-shaped bodies, which are typical of lateral accretion processes (cf. Miall, 2014). The lateral accretion deposits in the study area are generally up to 5 m thick and at least 700 m in length. Strata with this architectural element commonly show low-angle inclination

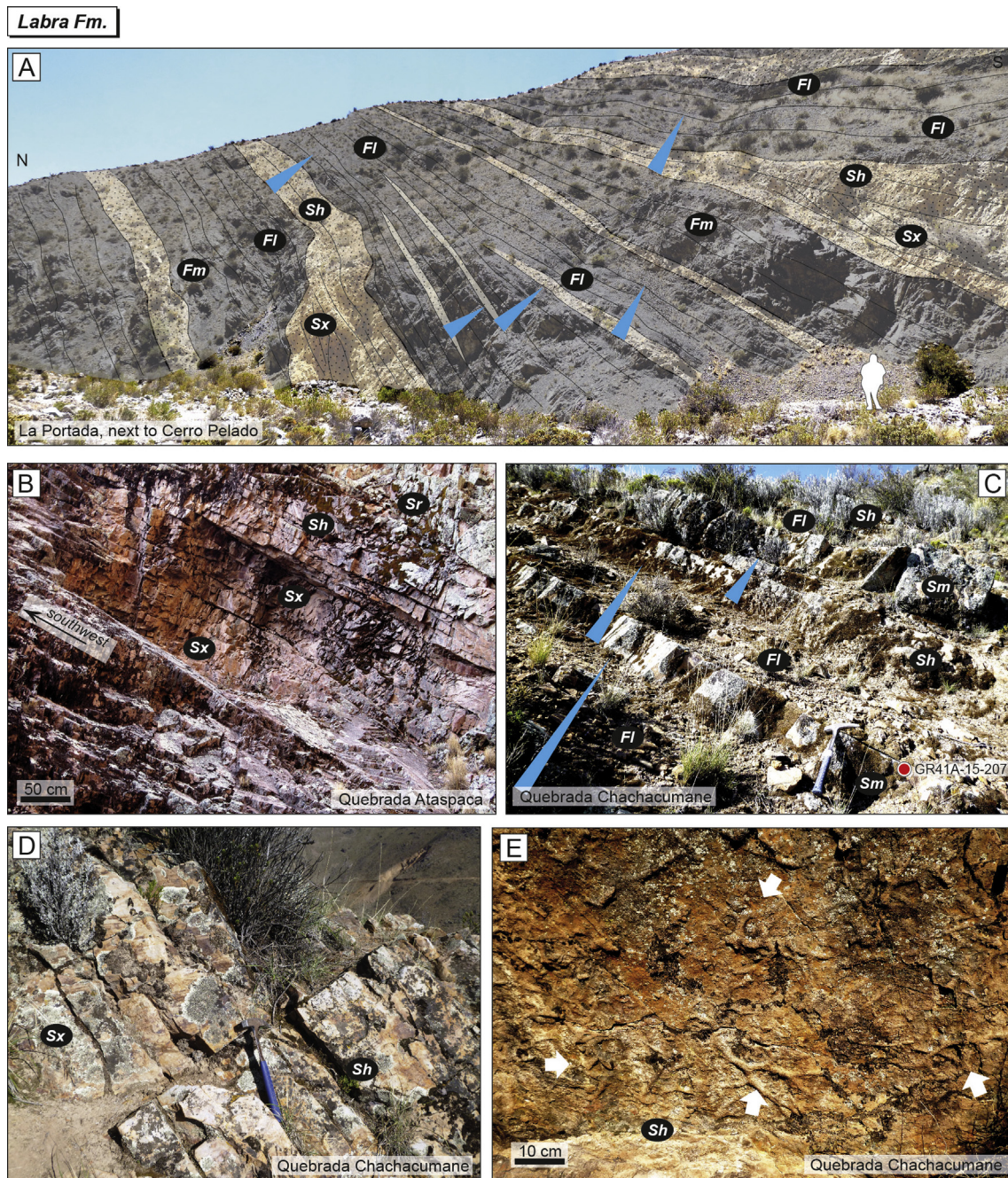


Fig. 8. Outcrops of sedimentary rocks of the Labra Formation in Tacna. In A: Massive sandstones and oblique stratification (*Sm*, *Sh* and *Sx* facies), interbedded with dark grey claystones of *Fl* and *Fm* facies. In B: Sequences composed of cross- and horizontal-laminated sandstones (*Sh* and *Sx* facies), showing *Sr* facies at the top of the sequences. In C: Fining-upward sequences from sandstones of *Sm* and *Sh* facies to dark grey sediments of *Fl* facies. In D: Fining-upward sequences containing cross-stratified and laminated sandstones (*Sx* and *Sh* facies). In E: Fine- to medium-grained sandstones of the *Sh* facies, with ichnofossils similar to *Thalassinoides*. See stratigraphic position of the photos within the Fig. 6.

(5°–25° at maximum) and are dominated by fining-upward packages of coarse- to fine-grained sandstones of the facies *Sx*, *Sr* and *Sh*. Finer grained lithofacies are generally observed at the base of the deposits with element *LA*, i.e. *Sr* facies. Commonly, the strata forming the *LA* element are commonly capped by very fine-grained sediments, such as dark grey claystones and siltstones of *Fm* and *Fl* facies (architectural element *FF*, see Section 5.5), which also appear as extensive tabular deposits (Fig. 8A and C). The *LA* element also occurs as large-scale planar sets with bounding surfaces dipping parallel to the channel axis.

The large-scale inclined strata and their bounding surfaces are produced by lateral migration (sedimentary accretion) of high-sinuosity sandy channels. These are indicative of lateral migration of sediments

that occurs typically in a point-bar deposit of a meander system (e.g. Allen, 1982), but also within a tidal system (cf. Davis, 2012) (see Section 7.1 for further information). Overall, the deposits of *LA* elements are larger and more common than their downstream-oriented counterparts of the *CH* elements. The *LA* element seems to be a larger-scale version of the *SB* element. Deposits with the *LA* element are observed widely along the Labra Formation, and often within the Cachíos Formation.

5.2.2. Interpretation

The *LA* elements are interpreted as having been deposited under a constant flow regime during normal river discharge and likely represent

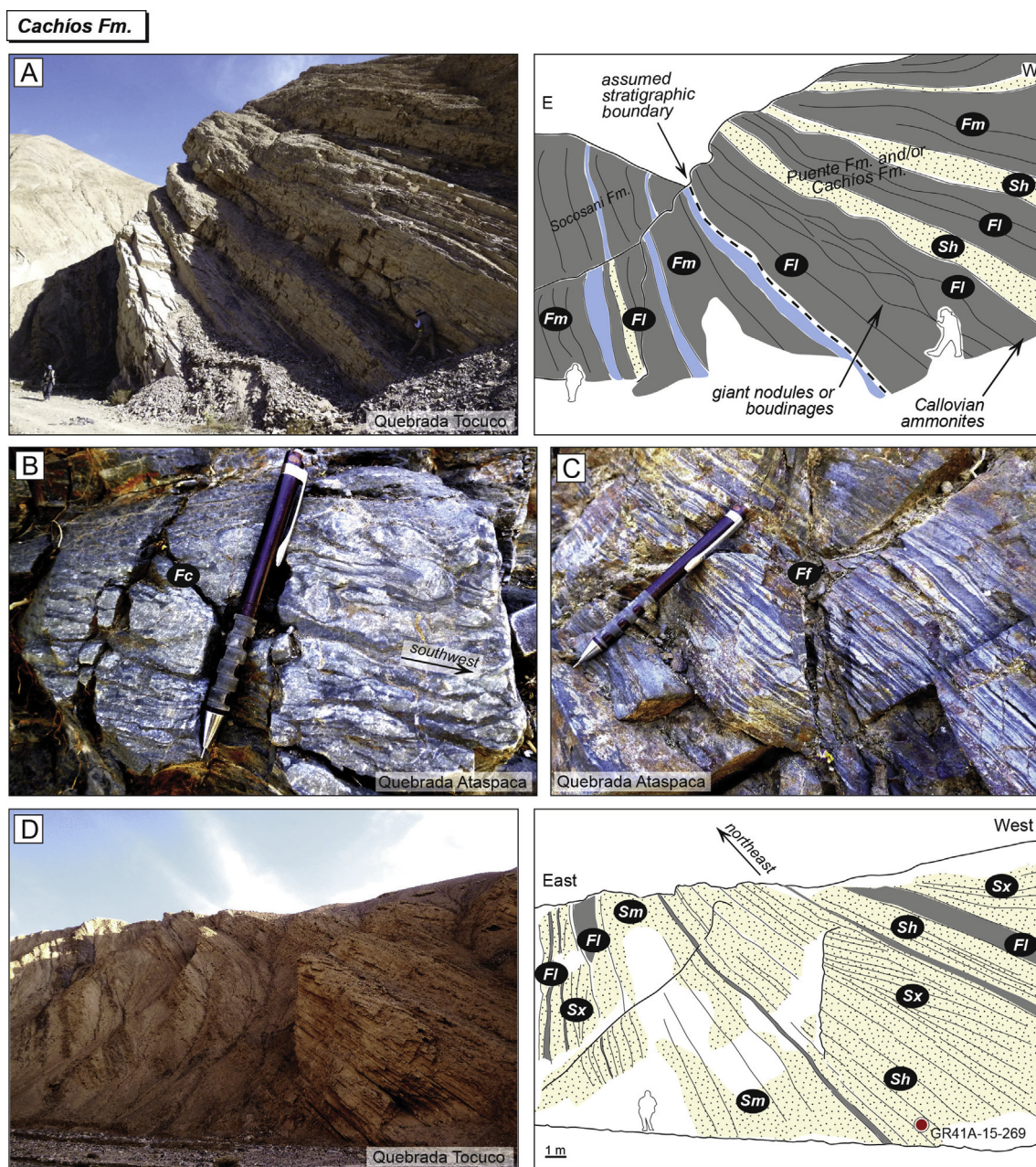


Fig. 9. Exposures of sedimentary rocks of the Cachíos Formation in Tacna. In A: Laminated claystones and siltstones (*Fm* and *Fl* facies) interbedded with minor fine-grained sandstones (*Sh* facies). In B: Black claystones and siltstones showing abundant flaser bedding (*Ff* facies). In C: Laminated black claystones of *Fl* facies. In D: Parallel-laminated sandstones (*Sh* facies) and cross-stratified sandstones (*Sx* facies), which commonly decrease to fine-grained sediments (*Fm* and *Fl* facies). In E: Deformed black claystones with convolute structures like "slumping". See stratigraphic position of the photos in the Fig. 6.

successions of mid-channel transverse bars within the central parts of a sinuous channel (e.g. Smith et al., 1989). Because of the occurrence of well-developed laterally extensive cross-bedded sandstones and ripple marks (at the surface) (cf. Miall, 2014), we suggest LA elements with large-scale inclined macroforms as representative of typical components of a point-bar. This interpretation is also supported by their thicknesses up to 5 m, and their paleocurrent orientations, which are commonly consistent with the mean paleoflow within the main channel body (e.g. Roberts, 2007). According to Allen (1970) and Miall (1985), strata displaying low-angle-inclined bounding surfaces (epsilon cross-bedding arising through a strong lateral component of bar migration relative to the main channel orientation and flow direction) indicates the migration of the channel via the deposition on the inside bends of sinuous meander curves. Moreover, the relative abundance of different

sedimentary structures at the topmost part of the deposits with LA elements changes laterally in response to varying channel sinuosity. Internal sedimentary structures (i.e. cross laminations and ripples marks of facies *Sx* and *Sr*) appear upward in order of declining flow power.

The vertical variations within the point-bar from sandstone and finer-grained sediments represent the "plug" of the channel, and are indicative of abrupt abandonment, either by avulsion or cut-off. The relative dominance of large-scale lateral accretion elements (ca. 700 m in length) over components similar to downstream accretion elements suggests a fluvial system dominated by laterally-accreting, sinuous bedload dominated channels. This condition suggests that the channels underwent high rates of lateral migration through the development of point bars on inner channel banks (cf. Miall, 1985). The deposits with

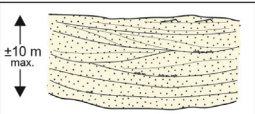
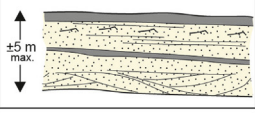
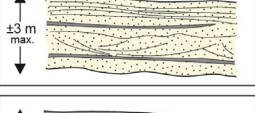
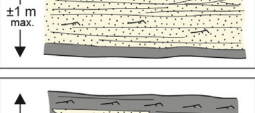
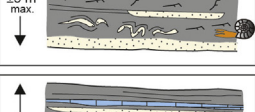
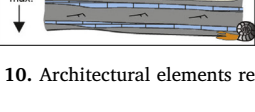
Architectural elements	Code	Lithology, sedimentary structures and fossils	Facies associations (FA)	Depositional environment
Channel	CH		Sx, Sm, Sh, Sr	Broad and lateral extension of listed facies, which indicates that these sand bodies arose via lateral (or downward) migration of the active part of the channel through the development of point-bars.
Lateral accretion	LA		Sx, Sr, Sh, FI	Deposition occurs by more than one laterally accreting sinuous, bedload-dominated fluvial system, which underwent high rates of lateral channel migration through the development of point-bars on inner channel bends.
Sandy bedform	SB		Sh, Sr, Sx	Deposition and accumulation of sediments occurs via migratory dune-scale bedforms in either on the flank of point-bars or even on mid channel bars.
Laminated sand sheet	LS		Sh, Sm, FI	Deposition occurs as bar top or bank flank sand sheets, which commonly accumulated in the shallowest parts of the channels.
Flood plain	FF		Fm, FI, Ff	Floodplain deposits with intercalated palaeosol units. Deposited over a wide area that was distal to the main channel in a semi-arid, oxidizing environment. Flaser bedding, slumps and convolute laminations are observed. Rarely marine fossils are present when associated to slumps.
Shallow sea	SS		Cca, Fca, FI, Sh, Ff	Deposited as coarsening-upward sequence capped by organic rich mudstones in shallow seas. Dark grey siltstones and very fine-grained sandstones are common. Often marine fossils are present.

Fig. 10. Architectural elements recognized in the Mesozoic sediments of Tacna.

LA elements are intimately related to the element CH (refer to Section 5.1).

5.3. Sandy-bedform elements (SB)

5.3.1. Description

These elements consist of tabular to wedge-shaped lenticular bodies up to 3 m thick (on its thickest side, otherwise is 2 m thick). The deposits with SB elements extend laterally for over 50 m with the largest bodies being located along the western flank of Cerro Chulluncane. The SB element is featured by stacked sandstones arranged into slightly inclined fining-upward packages with oblique trough and planar cross-stratified sets (facies Sx and Sh). The topmost deposits with SB elements are often capped by some rippled facies (i.e. facies Sr). The paleocurrents of such sedimentary structures usually exhibit different directions (e.g. south-westward, southward and often northward), similar to those measured for LA elements. Sandy bedforms of the SB element pass up section into very fine-grained sandstones of Sh facies, and are rarely overlain by floodplain black claystones and/or siltstones (either facies Fm or FI). The SB element seems to be a smaller-scale version of the LA element. Deposits with the SB element commonly occur within the Labra Formation.

5.3.2. Interpretation

The SB element represents the deposition of migratory dune-scale bedforms in either mid-channel bars or on the flanks of sand bars (which can be either point-bars or tidal bars), or even next to the channels (e.g. Allen, 1963; Miall, 1985; Hughes, 2012). The 50 m-long inclined macroforms represent fragments of point-bar lateral accretion deposits (cf. Roberts, 2007), or simply a minor-scale lateral accretion deposit within a fluvial context (as occur in LA elements, see Section 5.2). This interpretation is based on their length, size and orientation, which is subnormal to the mean palaeoflow within the main channel body, as suggested by local paleodirections from facies Sx and Sh.

Accordingly, each deposit with this element shows unidirectional indicators of a highly dispersive palaeocurrent trend, where the presence of lateral accretion macroforms and the fining-upward trend indicate that SB elements were deposited by small-scale meandering stream channels (e.g. Roberts, 2007).

5.4. Laminated sand sheet elements (LS)

5.4.1. Description

Deposits with this architectural element consist of up to 1 m thick strata. They occur as discontinuous tabular sheets of medium-to fine-grained sandstones that are commonly laminated (facies Sh) and rarely massive (facies Sm). Generally, this element contains inter-laminated black siltstones (facies FI), commonly appearing parallel and horizontal. The lamination is usually laterally continuous for about 20 m and sometimes exhibits primary current lineation on exposed bedding surfaces. This element is widespread throughout the lower part of the Yura Group, and it is closely associated with the FI facies (see Section 5.5 for further details).

5.4.2. Interpretation

Deposits including LS elements are interpreted as bar-top or bar-flank sand sheet deposits (Miall, 1985, 2014). The laminated deposits are discontinuous, non-channelized and show sheet-like geometry, together with small-scale sedimentary structures and widespread fine-grained lithology. Locally, the close association of LS elements with underlying channel bounding elements suggests that the sand sheets were also deposited rapidly by overbank sheet flows of very fine-grained sediments (similar to elements FF, see Section 5.5) rather than proper sheet floods. The cause of LS element may be attributed to two principal processes: (i) wave-swash and (ii) upper-flow regime plane beds. The first process likely occurred during a relative fall of the sea level, when large bedforms were accumulated by waves breaking over them as they emerged. Alternatively, laminated sand sheets attributed

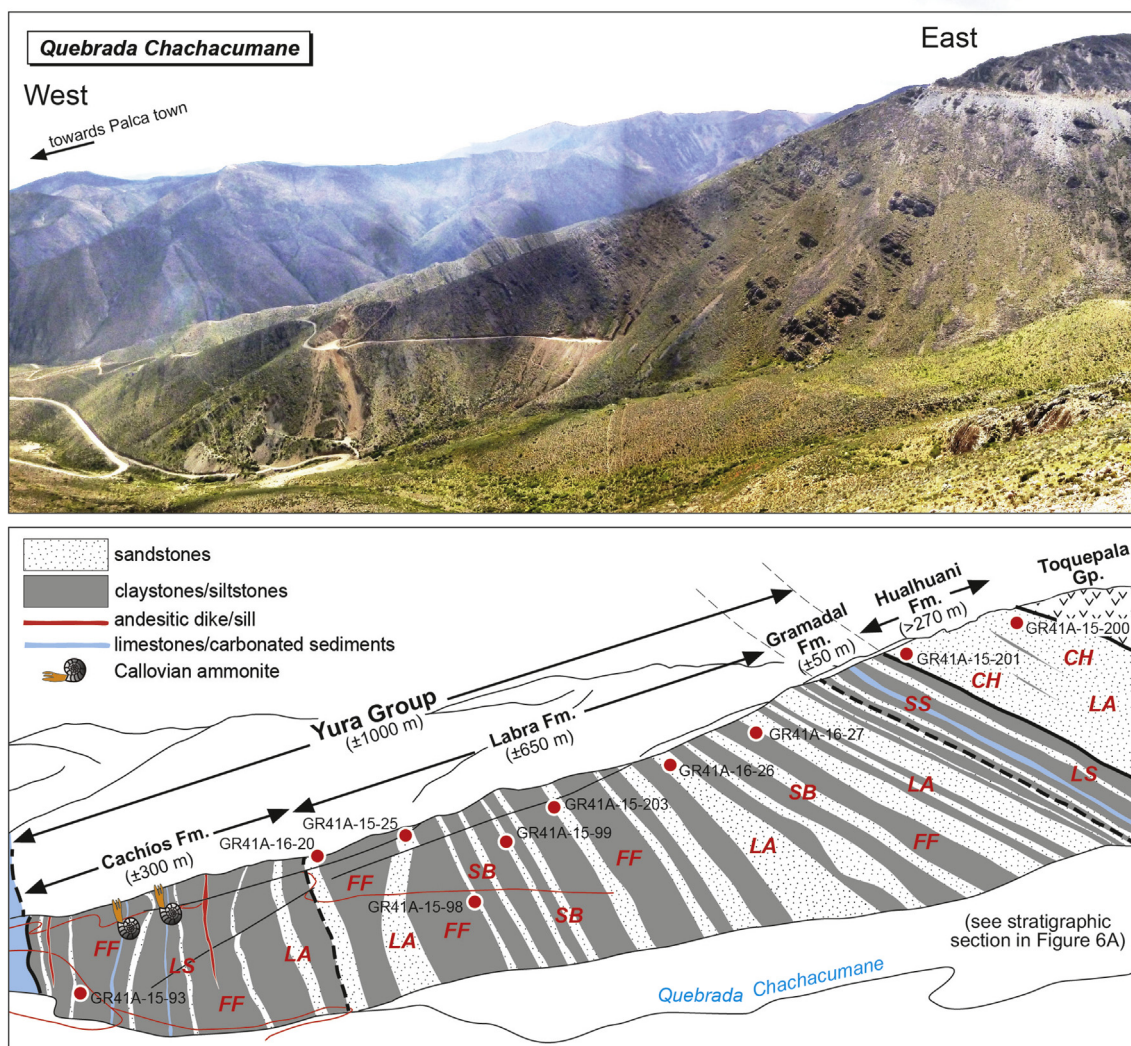


Fig. 11. Schematic diagram of the stratigraphic arrangement at the stratotype of the Mesozoic sediments in Tacna (Quebrada Chachacumane). We propose a new stratigraphic organization shown in this figure. Red circles indicate sampling of the sandstones for modal composition analysis. The stratigraphic section of Quebrada Chachacumane begins at UTM WGS84 E403646, N8036712 (near Copapuquio). (For interpretation of the references to colour in this figure legend, the reader is referred to the web version of this article.)

to upper-flow regime plane bed conditions may have developed in shallow water on the upper parts of the point-bar deposits (cf. [Plint, 1983](#)).

5.5. Floodplain elements (FF)

5.5.1. Description

The FF architectural element consists of 0.5–5 m-thick alternations of fine-grained black claystones (facies *Fm* and *Fl*). Such facies are commonly interbedded with dark grey siltstones and/or with quartzose fine-grained sandstone of the *Sx*, *Sm* and *Sh* facies. This sandy portion commonly shows an overall tabular and sheet-like geometry, and can correspond to the elements *LA*, *LS*, and *SB*. The deposits with FF elements (and the cited associated elements) can be observed laterally for distances of over 7 km, as for instance in Cerro Chachacumane. The most prominent feature of the FF element is the presence of massive-bedded deposits of *Fm* facies showing weak parallel laminations and occasionally concretions of up to 1 cm diameter ([Fig. 8A](#)). These beds usually contain very thin reddish layers disappearing laterally. When present, these layers are 40–50 cm thick, and usually comprise fossil plants fragments (leaves and stems) and horizontal burrowing (trails of ichnofossils similar to *Thalassinoides*). The deposits with the FF

architectural element also include desiccation cracks (if correspond to facies *Fl*) as well as a mix of black siltstone and white quartzose fine-grained sandstone (*Sx* facies). To increasing amounts of sand, generally follow the formation of both lenticular and flaser bedding (*Ff* facies, [Fig. 9C](#)). Laminae or lenticular structures of the FF elements are often deformed displaying convolute structures or slumped stratification ([Fig. 9B](#)).

Fine-grained carbonate sediments are commonly found within the FF element, and are defined here as the *Fca* facies (as defined in Section 4.9). At glance, the *Fca* facies is very similar to the adjacent facies *Fl* and *Fm* of the FF element; nonetheless, there are numerous features that allow a good differentiation among them. The fine-grained *Fca* facies are mixtures of carbonate and siliciclastic components including Callovian ammonites, and usually they are associated to slumps and flaser/lenticular bedding. The occurrence of the *Fca* facies within deposits of the FF element is not common, and occur only in few strata. The deposits with FF elements are very common within the Cachios and Labra formations. The *Fca* and *Cca* facies are included within the SS architectural element (see Section 5.6).

5.5.2. Interpretation

The origin of deposits with the FF element is to be attributed to the

excess of fluvial discharge, where siltstones and claystones overbank (facies *Fm* and *Fl*). The fine grain size and the extensive tabular and sheet-like geometry of these elements indicate deposition over a wide area that was adjacent and/or distal to/from the main channel. The accumulation of particles mostly concentrated in the floodplain (or even swamp) deposits or may have happened within “depressions” which are commonly extensive and flat enough to receive such amount of sediments (cf. Víseras & Fernández, 2010). The intermittent thin layers of sandstones (e.g. facies *Sx* and *Sh*) may correspond to laminar sheet-floods deposited away from the main channel, or simply to lateral migration of point-bars deposits. The development of desiccation cracks indicates fluctuating wet to dry conditions at the surface. The occurrence of oxidizing near-surface conditions (some minor reddish layers) is also supported by the absence of carbonaceous root material in those layers. The common presence of fossil plants within those fine-grained sediments is indicative of a humid environment with abundant vegetation.

Carbonate facies (i.e. *Fca* facies) are often associated to deposits with the *FF* element and may suggest marine influence (e.g. tidal). Nonetheless, some of the carbonate particles may as well occur in fine-grained deposits of continental environments (cf. Freydet and Plaziat, 1982) (see Section 8.1. for further discussions). The marine influence is confirmed by the presence of ammonites (either Callovian or Tithonian), which are commonly associated to slumps and flaser bedding (*Ff* facies) (see Section 5.6 for further details). In this context the *FF* element can be also associated to the *SS* architectural element.

5.6. Shallow sea elements (*SS*)

5.6.1. Description

The architectural element *SS* represents sedimentary deposits accumulated in shallow sea environments. The *SS* elements comprises internal beds with the facies *Cca* and *Fca*, and are often interbedded with subordinate facies of *Fm*, *Fl*, *Sr* and *Sh*. We divide the *SS* element into two main parts, (i) the coarse-grained (*Cca* facies) and (ii) the fine-grained (*Fca* facies) dominated deposits. When occurring, the deposits dominated by the *Cca* facies are typically 1 m thick; and they can group into sets of up to 5 m thick, extending for more than 3 or 4 km width. The deposits dominated by the *Cca* facies, consist of internal beds of carbonate claystone that varying in thickness between 30 and 40 cm and are commonly interlayered with sandstone beds of the *Sh* facies and laminated claystones and/or siltstones of *Fl* facies. It is common to observe tractive structures as ripple marks (*Sr* facies). Together, these beds form fining-upward sets of up to 5 m thick, with the *Cca* facies at the bottom and the *Sr* facies at the top. The *Cca* facies commonly contain Tithonian ammonites associated to fragmented molluscs and bivalves. These facies are particular abundant in the Cerro Challatita section (see Fig. 6D).

Frequently, the deposits dominated by the *Fca* facies have internal beds varying in thickness between 10 and 20 cm. Sediments of this facies are commonly associated to those of the *Fm* and *Fl* facies and rarely with those from facies *Sh* and *Sr*. Thin sandstone beds of the *Sh* facies are associated to *SS* elements and rapidly pinch-out laterally. Some ripple marks of *Sr* facies and desiccation cracks appears at the top of such lenticular deposits of sandstone. The deposits with dominant *Fca* facies are generally 50 m wide and form lenticular or sheet-like geometry pinching-out into surrounding laminated mudstones and/or claystones. These sediments occur as well within the Gramadal Formation of the Quebrada Chachacumane (see Fig. 6A) but do not contain Tithonian ammonites or associated molluscs. It is important to highlight that these facies are very similar to those described within the *FF* elements. The more relevant difference between the two is the carbonate content. This type of facies is also observed along the middle part of the Cachíos Formation (Quebrada Tocuco, Fig. 6C, and Quebrada Chachacumane, Fig. 6A), although, its occurrence is vertically limited. This carbonate facies in normally ammonite-bearing

(Callovian) and appear intimately associated to facies of the *FF* element (see Section 5.5).

5.6.2. Interpretation

The *SS* architectural element represents all sedimentary deposits accumulated in (or influenced by) shallow marine environments and containing carbonate deposits. The facies described above define at least two depositional sub-environments. In fact, the bioclastic coarse-grained limestone of the *Cca* facies (and associated facies) is typical of deposition of shallow carbonate platform under high-energy conditions (for instance, Cerro Challatita, cf. Quispe, 2016). This feature may also indicate a tidal (or intertidal) influence. The possible presence of marls and fine-grained sediments (e.g. facies *Fl* and *Sh*) may suggest episodes of gravity accumulation of suspended particles during slack waters conditions (cf. Davis, 2012).

The character of the *Fca* facies also indicates deposition by suspension in standing water in an extensive shallow marine environment (e.g. Fielding and Webb, 1996). In such condition, the gradual input of sand was likely carried into the basin via low-energy traction currents of local extension (possibly tidal deltas, cf. Hughes, 2012). Desiccation cracks and negligible wave ripples probably represent the marginal deposits of a shallow sea and subordinate influence of the tidal processes. On the other hand, the *Fca* and associated facies are also observed within strata of the Cachíos Formation, suggesting a shallow-marine environment or possibly an ephemeral muddy tidal flat. Layers with Callovian ammonites (see lower Cachíos Formation in Fig. 6A) are representative of marine environments of at least 50 m deep (Callovian Perisphinctids, cf. Westermann, 1996).

6. Modal composition of the Mesozoic sandstones (light minerals)

The modal framework compositions were obtained from the analysis of 27 moderately to well sorted fine-to coarse-grained sandstones. These samples were prepared for standard petrographic thin sections and analysed under petrographic microscope according to the parameters provided in Dickinson and Suczek (1979) and Ingersoll et al. (1984) (Table 1). 350 to 500 grains per thin section were counted according to the Gazzi-Dickinson method. Compositional data were recalculated to 100% (Table 2) and plotted into classification diagrams proposed by McBride (1963) (Fig. 12).

6.1. Petrofacies and interpretations

According to the first-order classification of arenites by Zuffa (1980), all samples in this manuscript are sandstones, and are composed predominantly of siliciclastic components. Following to the second order classification of McBride (1963), the majority of sandstones are quartzarenites, and subordinate sub-arkoses, arkoses and lithic arkoses. These arenites are coarse to fine-grained, moderately to well sorted.

6.1.1. Petrofacies in the Cachíos Labra and Gramadal Formations (Yura Group)

Quartz is the main constituent of the Yura Group arenites (97%), which are classified as quartzarenites, subarkoses and quartzwackes (Fig. 12A). The framework grains are composed predominantly of monocrystalline quartz (Qm), and subordinately of polycrystalline (Qp) and undulating (Qo) grains. Feldspar grains occur in more than half of the samples; although in low amounts (8.4–21.7%). K-feldspars are monocrystalline while plagioclase shows polysynthetic twinning. Both minerals show advanced stages of weathering/diagenetic overprint consisting of kaolinite and sericite respectively. Plagioclase grains occur only within the Cachíos Formation and the lower Labra Formation. Lithic fragments are rare throughout the Yura Group, and are primarily of volcanic composition (Lv, 0.2% and 13.9% on total framework composition) and exhibit a microcrystalline texture. Accessory minerals

Table 1
Compositional framework of the Mesozoic sediments of Tacna. The column “others” includes heavy minerals.

N°	Sample	Lithology	Locality	Unit	Qm	Qo	Qp	Fp	Fk	Lv	Ls	Lm	others	Total	Q	F	L	Qt	F	It
1	Low sinuosity (Hualhuani Fm.)	Quartzarenite	Cerro Challatita	Hualhuani Fm.	68.1	17.3	11.1	0.0	0.3	0.0	0.0	0.6	2.6	342	99.1	0.3	0.6	99.1	0.3	12.0
2	GR41A-15-279	Quartzarenite	NE Ataspaca	Hualhuani Fm.	89.6	8.3	1.1	0.0	0.4	0.4	0.0	0.0	0.4	278	99.3	0.4	0.4	99.3	0.4	1.4
3	GR41A-15-200	Quartzarenite	E Copapuquio	Hualhuani Fm.	72.3	11.2	15.7	0.0	0.0	0.0	0.0	0.0	0.8	357	100.0	0.0	0.0	100.0	0.0	15.8
4	GR41A-15-101	Subarkose	E Copapuquio	Hualhuani Fm.	67.4	18.1	6.3	1.0	5.3	1.0	0.2	0.0	0.8	509	92.5	6.3	1.2	92.5	6.3	7.5
5	GR41A-16-28	Quartzarenite	Qda. Chachacumane	Hualhuani Fm.	82.4	14.8	1.5	0.0	0.0	0.5	0.0	0.0	0.8	391	99.5	0.0	0.5	99.5	0.0	2.1
6	GR41A-15-201	Quartzarenite	Qda. Chachacumane	Hualhuani Fm.	62.9	20.6	10.4	0.0	0.0	0.0	0.0	0.0	5.2	364	99.1	0.0	0.9	99.1	0.0	11.9
7	High sinuosity (eanders (Yura Group)	Quartzarenite	Cerro Challatita	Gramadal Fm.	73.9	7.2	9.4	0.0	3.6	1.8	0.0	0.0	4.0	445	94.9	3.4	1.7	94.9	3.4	10.7
8	GR41A-15-276	Subarkose	Cerro Challatita	Labra Fm.	68.0	11.7	12.5	0.0	5.4	1.7	0.0	0.0	0.6	463	92.8	5.4	1.7	92.8	5.4	14.3
9	GR41A-16-80	Quartzarenite	Cerro Tocuco	Labra Fm.	76.6	9.1	5.5	0.0	4.8	2.4	0.0	0.0	1.7	418	92.7	4.9	2.4	92.7	4.9	8.0
10	GR41A-15-102	Subarkose	Qda. Chachacumane	Labra Fm.	67.8	11.1	6.3	0.0	8.4	1.9	2.9	0.0	1.7	478	86.6	8.5	4.9	86.6	8.5	11.3
11	GR41A-15-274	Quartzarenite	Cerro Challatita	Labra Fm.	83.3	3.6	9.3	0.0	0.0	3.0	0.0	0.0	0.8	365	97.0	0.0	3.0	97.0	0.0	12.4
12	GR41A-15-206	Quartzarenite	E Ataspaca	Labra Fm.	76.2	11.0	8.0	0.0	0.0	0.0	0.0	1.1	3.7	462	98.9	0.0	1.1	98.9	0.0	9.4
13	GR41A-16-84	Quartzarenite	Cerro Tocuco	Labra Fm.	80.8	14.5	3.7	0.0	0.0	0.0	0.0	0.0	1.0	704	100.0	0.0	1.0	100.0	0.0	3.7
14	GR41A-15-49	Quartzarenite	Cerro Tocuco	Labra Fm.	82.2	5.6	6.2	0.0	3.0	1.1	0.0	0.0	1.9	533	95.8	3.1	1.1	95.8	3.1	7.5
15	GR41A-16-82	Quartzarenite	Cerro Tocuco	Labra Fm.	78.6	14.2	4.6	1.1	0.0	0.5	0.0	0.0	1.1	569	98.4	1.1	0.5	98.4	1.1	5.2
16	GR41A-16-32	Quartzarenite	E Ataspaca	Labra Fm.	80.4	7.4	9.9	0.2	0.0	1.0	0.0	0.0	1.2	514	98.8	0.2	1.0	98.8	0.2	11.0
17	GR41A-16-27	Quartzarenite	Qda. Chachacumane	Labra Fm.	80.7	5.8	10.6	0.4	0.0	0.0	0.0	0.0	2.5	566	99.6	0.4	0.0	99.6	0.4	10.9
18	GR41A-16-26	Quartzarenite	Qda. Chachacumane	Labra Fm.	81.7	9.7	7.4	0.6	0.0	0.0	0.0	0.0	0.7	725	99.4	0.6	0.0	99.4	0.6	7.5
19	GR41A-15-99	Quartzarenite	Qda. Chachacumane	Labra Fm.	80.6	3.9	11.7	0.0	3.2	0.2	0.5	0.0	0.0	571	96.1	3.2	0.7	96.1	3.2	12.4
20	GR41A-15-203	Quartzarenite	Qda. Chachacumane	Labra Fm.	84.3	4.3	9.1	0.0	0.0	1.0	0.0	0.0	1.3	394	99.0	0.0	1.0	99.0	0.0	10.3
21	GR41A-15-98	Subarkose	Cerro Tocuco	Labra Fm.	85.6	1.1	1.7	5.0	1.0	5.6	0.0	0.0	0.0	178	88.5	6.0	5.6	88.5	6.0	7.3
22	GR41A-15-95	Quartzarenite	Qda. Chachacumane	Labra Fm.	33.3	49.1	16.6	0.1	0.6	0.0	0.1	0.0	0.1	727	99.2	0.7	0.1	99.2	0.7	16.8
23	GR41A-15-211	Quartzarenite	E Ataspaca	Labra Fm.	83.2	7.0	3.8	0.0	2.4	3.5	0.0	0.0	0.0	370	94.1	2.4	3.5	94.1	2.4	7.3
24	GR41A-16-25	Quartzarenite	Qda. Chachacumane	Labra Fm.	82.2	5.4	8.7	0.2	0.0	2.2	0.0	0.0	1.3	461	97.6	0.2	2.2	97.6	0.2	11.0
25	GR41A-15-187	Quartzarenite	Qda. Chachacumane	Cachíos Fm.	73.9	10.0	8.6	0.0	0.8	2.5	0.0	0.0	4.2	479	96.5	0.9	2.6	96.5	0.9	11.5
26	GR41A-15-269	Arkose	Cerro Challatita	Cachíos Fm.	43.5	10.4	2.6	21.7	7.0	13.9	0.0	0.0	0.9	115	57.0	28.9	14.0	57.0	28.9	16.7
27	GR41A-15-93	Quartzwacke	Qda. Chachacumane	Cachíos Fm.	82.0	10.1	2.2	0.0	4.9	0.3	0.3	0.0	0.3	366	94.5	4.9	0.5	94.5	4.9	2.7

Table 2
Framework parameters used in this study (after Dickinson and Suczek, 1979).

Quartz grains ($Q_t = Q_m + Q_p$)	
Q_t = total quartz grains where	
Q_m = monocrystalline quartz	
Q_p = polycrystalline quartz including chert	
F = total feldspar ($F_k + F_p$), where	
F_k = potassic feldspar	
F_p = plagioclase	
R = rock fragment including chert fragments	
<hr/>	
Qm-F-Lt	
Q_m = monocrystalline quarts	
F = total feldspar	
L_t = lithic fragments + Q_p	

include amphibole, pyroxene, zircon, rutile and garnet (cf. Trinidad, 2017).

Both textural and compositional maturity of analysed sandstone samples indicate recycling from a cratonic source, and best represents the main supply of sediments for the Yura Group (Fig. 12D). Nonetheless, if these sedimentary facies were exposed to a highly humid

climate (see Section 7.1 for further information), the provenance might reflect a closer source. For instance, Ochoa et al. (2007) and Caracciolo et al. (2009) suggested that a dominant amount of Qt and reduced proportions of detrital feldspars (in a similar rift basin-fill) is attributed to an intense chemical weathering of a tropical climate. However, the typical rounded nature of quartz grains together with the lack of clayey matrix allow excluding this option as intense alteration, because alone would not be sufficient to determine such textural features.

On the other hand, there are proportions of volcanic lithic fragments and feldspars (although very low), suggesting erosion of volcanic rocks (e.g. Chocolate Formation) and some influence from an uplifted basement. Such proportions (0.5–13.9%) are typical of the lower Yura Group (Cachíos Formation), and gradually disappear upward possibly reflecting a gradual change of the drainage system.

6.1.2. Petrofacies in the Hualhuani Formation

Sandstones of the Hualhuani Formation classify as quartzarenites and represent the quartz-richest sediment fill of the Mesozoic Arequipa Basin (Fig. 12B). The Q_m and Q_o values are higher than those observed in the arenites of the Yura Group (89.6% and 20.6%, respectively). Feldspar grains are scarce (values between 0.3 and 1.0%), generally monocrystalline and very altered and/or partially dissolved. Lithic fragments are also rare, and are only found in two samples (0.4% and

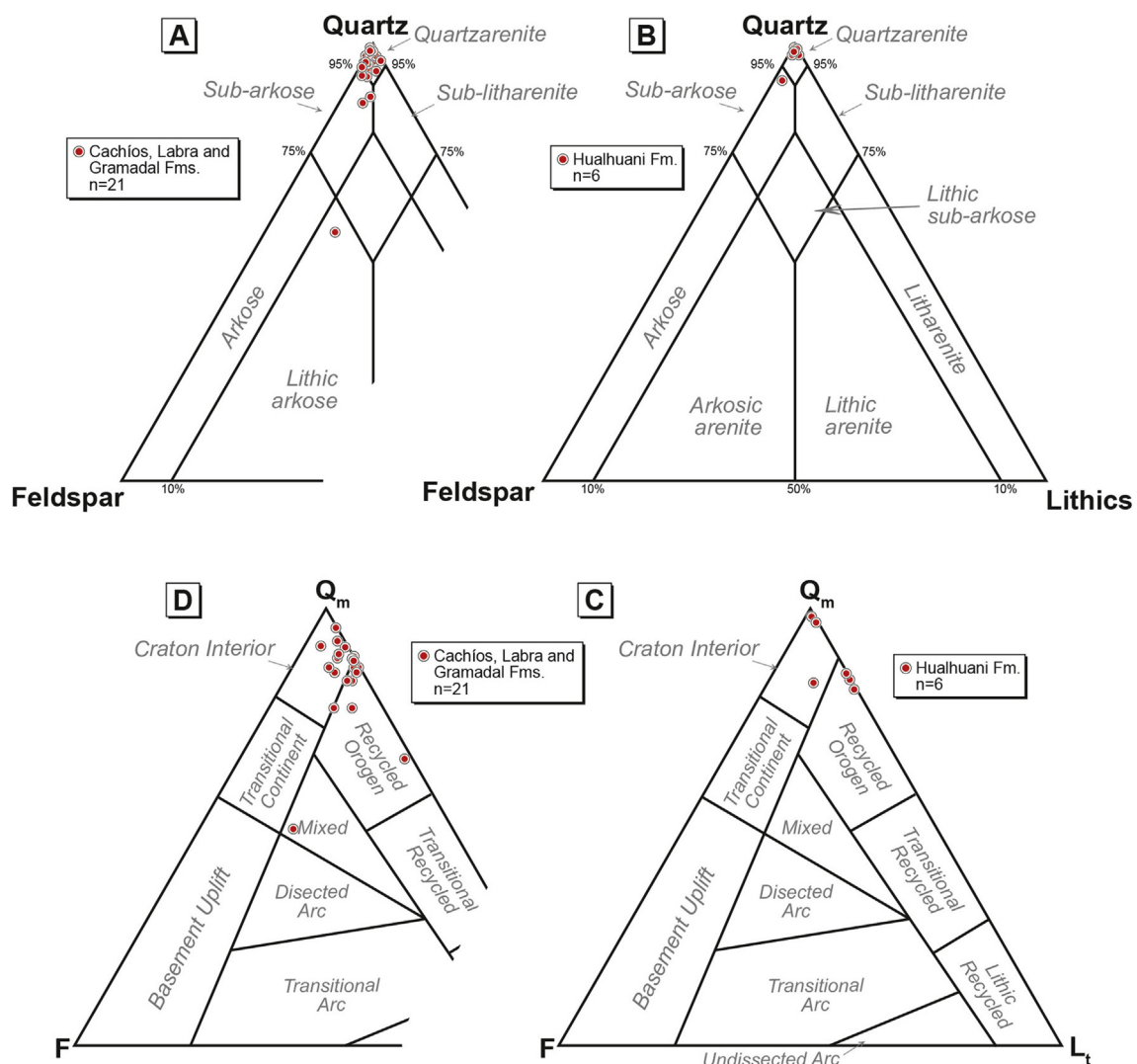


Fig. 12. The classification of Mesozoic sandstones is based on light mineral data. In A and B: Q-F-L diagrams for classification of arenites introduced by McBride (1963). In B and C: Representation of the light mineral data within the QmFLt tectonic provenance diagram proposed by Dickinson et al. (1985).

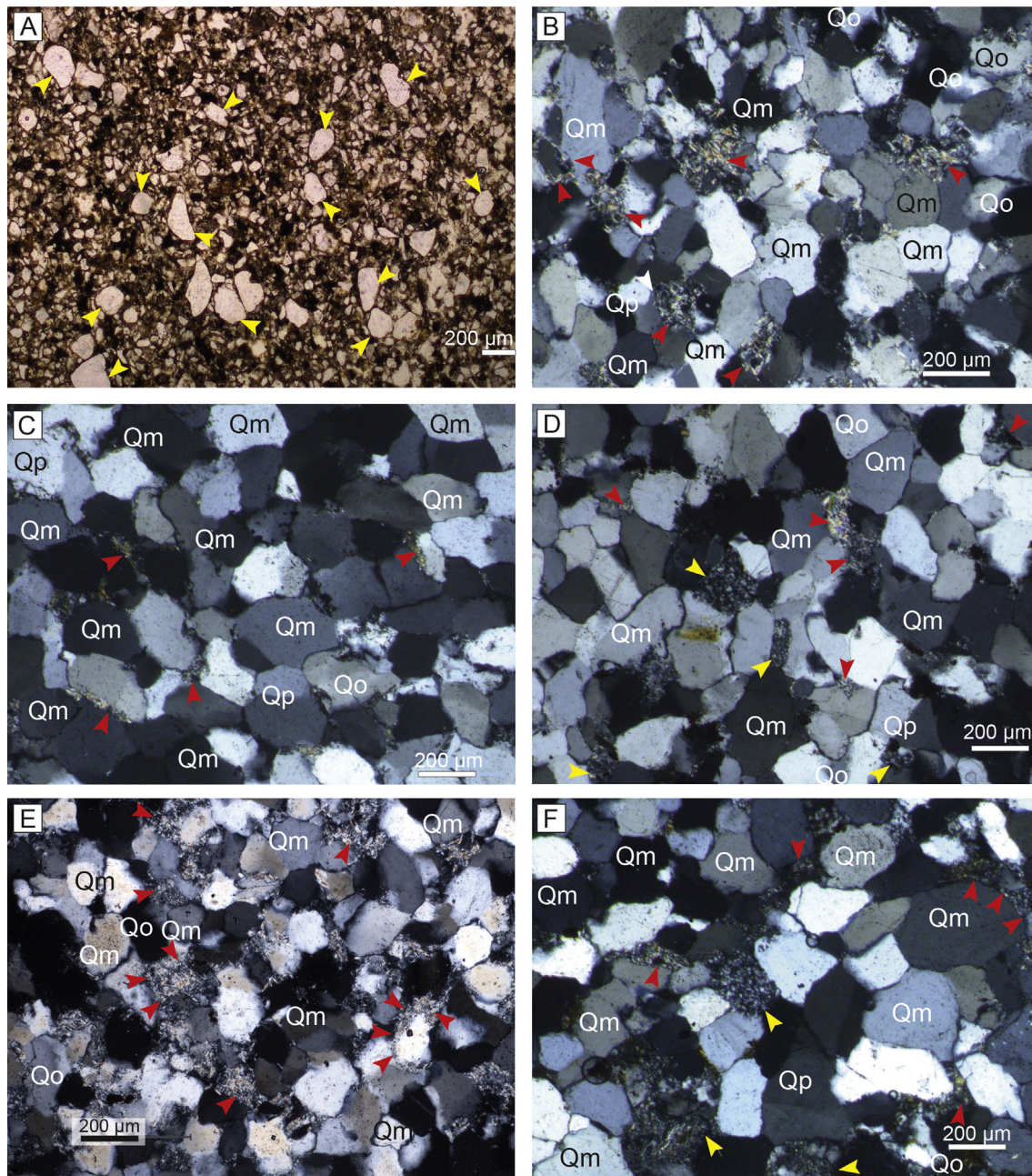


Fig. 13. Photomicrographs of the main lithofacies of the Mesozoic sediments in Tacna. In A: Fine- to medium-grained quartzwacke of the lower Cachíos Formation (sample GR41A-15-93, *Sh* facies). Note the remarkable proportion of clay/siltstone matrix. Most of the grains are monocrySTALLINE quartz (yellow arrows). Plane polarized light. In B: Medium-grained quartzarenite of the upper Cachíos Formation (sample GR41A-15-187, *Sr* facies). Note the cementation of phyllosilicate components (red arrows). Crossed nicols. In C: Medium-grained quartzarenite of the middle Labra Formation (sample GR41A-16-32, *Sm* facies). Crossed nicols. In D: Medium-grained quartzarenite of the upper Labra Formation (sample GR41A-15-206, *Sr* facies). Crossed nicols. In E: Medium-grained subarkose of the lower Hualhuani Formation (sample GR41A-15-102, *Sh* facies). Note the significant amount of phyllosilicate cementation (yellow arrows). Crossed nicols. In F: Medium-grained quartzarenite of the upper Hualhuani Formation (sample GR41A-15-279, *Sx* facies). Crossed nicols. Abbreviations: Qm = monocrySTALLINE quartz, Qp = polycrySTALLINE quartz, Qo = undulating quartz. (For interpretation of the references to colour in this figure legend, the reader is referred to the web version of this article.)

1.0%). Some notable accessory minerals include zircon, rutile and tourmaline (ZTR, cf. [Trinidad, 2017](#)).

The extremely Qm-rich arenites of the Hualhuani Formation are also consistent with the denudation of a cratonic source (cf. [Dickinson and Suczek, 1979](#); [Dickinson et al., 1985](#)) (Fig. 12D). Similar to the underlying Yura Group, the maturity of these arenites is very possibly due to continuous sedimentary reworking and recycling. Further evidences supporting the dominance of multi-cycle sedimentation is reinforced by the presence of ultrastable minerals (ZTR).

6.2. About the cementation

Cements in analysed sandstones samples consist mostly pore-filling and rimming authigenic phyllosilicates (Fig. 13) and are mostly concentrated in the lower Yura Group. The presence of clayey cements is consistent with the dominance of clays (architectural elements *FF*) as product of gravity sedimentation after lateral accretion processes.

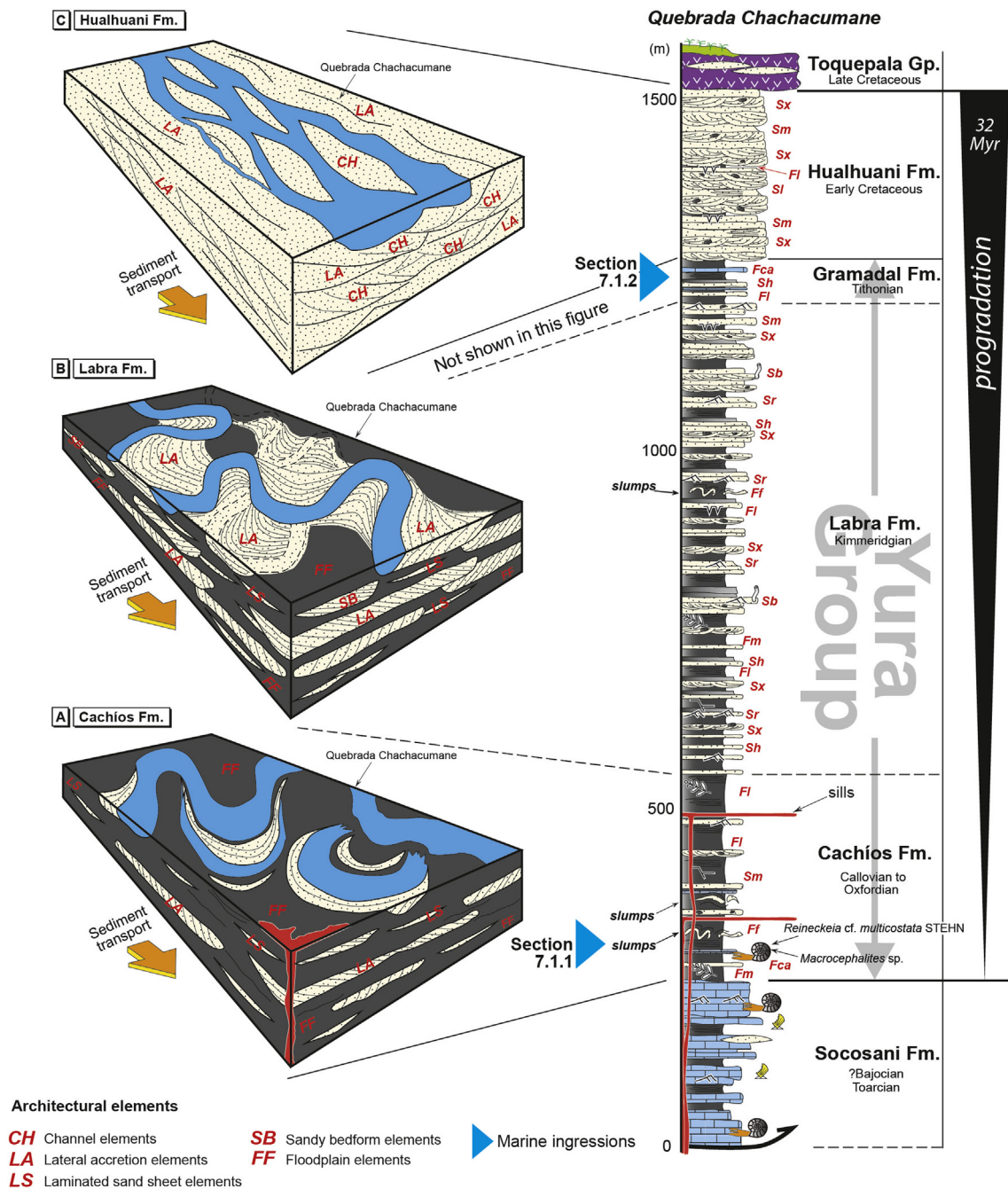


Fig. 14. Schematic representation of the two sedimentary environments interpreted for the Mesozoic sediments of Tacna (not to scale). In A and B: Establishment and development of meandering rivers and sedimentary deposition of the Cachíos Formation, with gradual increase of LA elements (Labra Formation). In C: Establishment of braiding deposition of the Hualhuani Formation (Berriasian). These depositional settings reflect the upward evolution of a meandering to braiding fluvial system in Tacna.

7. Sedimentary environments of the Arequipa-Tarapacá Basin-fill in Tacna and interpreted processes

The identification and sub-division of both sedimentary facies and architectural elements allowed to define two main depositional settings. Evidences allowing further sub-division of sub-environments provide elements for unravelling the sedimentary and geodynamic history of the Mesozoic Arequipa Basin. The Puente Formation s.s. is omitted due its absence, being the Cachíos Formation directly overlying the Socosani Formation. In contrast to Acosta et al. (2011), it is impossible to consider these sediments as the grouping “Puente-Cachíos Formation”, instead, it is adequate only as Cachíos Formation.

7.1. Meandering rivers of the Cachíos Formation (Callovian to Oxfordian) and the Labra Formation (Kimmeridgian)

The stratigraphic arrangement of the Cachíos Formation is characterised by a marked predominance of architectural elements FF and LS (and subordinately LA and SB) organized in cyclic sequences (Fig. 14A), suggesting at least three possibilities with respect to sedimentary environments: (i) a wide floodplain area across which a channel meandered, (ii) rapid floodplain deposition relative to the frequency of channel avulsion, or (iii) predominant growth of appreciable alluvial floodplain relief (cf. Nanson and Croke, 1992). Our observations are more consistent with (i) and (ii), since they better define

a floodplain area of a wide and semi-flat environment with high-sinuosity meanders, constant overbank processes, and rapid deposition of fine-grained sediments at the end of each cycle. The association of architectural elements is consistent with a model in which sediments of the Cachíos Formation accumulated within a highly-sinuosity meander system, where floodplain deposits (*FF* elements) were predominant. Such predominance may also be a consequence of rapid abandonment of a meander channel, confirming in this way its high-sinuosity character (cf. [Víseras and Fernández, 2010](#)).

Upward, *LA*, *LS* and *SB* elements become gradually predominant over the *FF* elements, and its stratigraphic organization mark the transition of the Labra Formation (650 m thick) (e.g. Quebrada Chachacumane, see [Fig. 11](#) for reference). Depositional features are remarkably uniform and typical of cyclic sedimentation (for instance, [Fig. 8C](#)), especially in the Labra Formation. The bottom of each cycle is inclined, and shows patterns reflecting extensive point-bar lateral migration developed on inner channel bends (facies *Sx*, *Sm* and *Sr*). Eventually abandonment and plugging of sediments with slack water deposits (facies *Sh* and *Sr*) pass to unconfined floodplain overbank sediments (facies *Fm* and *Fl*). All the facies and elements associated defined within the Labra Formation show the typical signature of multistory sandy deposits, reflecting a high-to moderate-sinuosity meandering complex (as depicted in [Fig. 14B](#)).

The sedimentary successions of the Cachíos and Labra formations are grouped in this section because their deposits reflect a gradual increase of the elements *LA* and *SB*, and correspondent decrease in the frequency and abundance of *FF* and *LS* elements, highlighting a marked progradational trend of fluvial nature (compare [Fig. 14A](#) and [B](#)). Nonetheless, evidences of marine influence exist and provide important information on specific geodynamic settings (see Sections [7.1.1](#) and [7.1.2](#)).

7.1.1. A marine ingressión during deposition of the Cachíos Formation

Evidences of marine sedimentation are recorded within the *Fca* facies of the Cachíos Formation. Such evidences have also been discussed by [Wilson and García \(1962\)](#) and [Westermann et al. \(1980\)](#) who reported Callovian ammonites e.g. *Reineckeia cf. brancoi* STEINMANN and *Reineckeia multicostata* STEHN, and *Macrocephalites cf. diadematus* WAAGEN DESTEHN). These ammonites have been described on the same facies exposed along the easternmost outcrops of the Province of Puno (69°W) by [Stehn \(1923\)](#) and [Aldana \(1989\)](#). The presence and meaning of such marine fauna can be related to (i) the proximity to a marine realm (marginal marine settings), and/or (ii) a strong pulse of subsidence that triggered to a marine ingressión extending as far as the region of Puno (as depicted in [Fig. 15](#)). We agree with both points and suggest in addition the simultaneous influence of a tectonic mechanism. Our facies analysis suggests the development of meander and floodplain deposition had to be developed on a semi-flat topography, proximal to (or through) a shallow-marine setting (or intertidal area), as proved by some Callovian perisphinctids reported in this study. The intensification of such tide oscillations and/or other associated phenomena, enough to allow the habitat of perisphinctids, must be a consequence of a tectonic subsidence (see further discussions in Section [8.3](#)).

7.1.2. A marine ingressión during deposition of the Gramadal Formation (Tithonian)

The Gramadal Formation s.s. of Arequipa consists of carbonate sediments and sandstones of 80 m of Tithonian age ([Benavides, 1962](#)). In Tacna, the strata of this unit show ca. 60 m thick as maximum (e.g. Cerro Challatita, [Fig. 4](#)) and become thin laterally until disappearing, leading a direct contact between the Labra Formation and the overlying Hualhuani Formation (e.g. near Ataspaca, [Fig. 3](#)). The exposures in Cerro Challatita consist of dominate coarse-grained carbonate sediments of *Cca* facies (rudstones, floatstones and grainstones) interbedded with sandstones and subordinate claystones and occasionally Tithonian ammonites (*Windhausenicerias* sp. And *Perisphinctes* sp., cf. [Wilson and](#)

[García, 1962](#); [Monge and Cervantes, 2000](#); [INGEMMET, 2016](#)) (see Cerro Challatita section in [Fig. 6D](#)). Conversely, fine-grained facies as claystones, carbonate sandstones, marls and often limestones of the *Fca* facies are found in Cerro Chachacumane. *Fca* facies are here interpreted as corresponding to a lateral change in facies from shallow marine to a more inland setting, especially considering the occasional presence of mudcracks. To increases in sandstones and claystones correspond the appearance and association with facies *Sm*, *Sh* and *Fl*.

The association of these facies allowed to introduce the *SS* architectural element, implying that existed favourable conditions during the deposition of the Gramadal Formation for the accumulation of carbonate particles through a marine ingressión, and consequent shift to a shallow-marine setting. As for the first marine ingressión (Middle Callovian), this other event also disrupted the typical signature of a progradational fluvial trend (see Section [8.3](#) for further discussions).

7.2. Braiding rivers of the Hualhuani Formation (Berriasian)

We agree on the interpretation from [Wilson and García \(1962\)](#) and [Monge and Cervantes \(2000\)](#) which identified in the dominance of sandy strata as the typical signature defining the Hualhuani Formation. In effect, the proportion of sandstones within the Hualhuani Formation contrasts widely with that observed within the Cachíos, Labra and Gramadal formations. The Hualhuani Formation is dominantly composed by sandstones typical of the *CH*, *LA*, and *SB* elements ([Fig. 14C](#)) (and rarely fine-grained sediments of the element *FF*) which occur as laterally extensive bars of more than 7 km in length. When fine-grained sediments of the element *FF* are present, they appear as small-scale lenticular strata laterally pinching-out (no more than 10 m wide). Sedimentological observations indicate that the erosive nature of the deposition of the elements *CH* and *LA* do not allow the deposition of the elements *FF*.

Deposits of the Hualhuani Formation are dominated by sandstones of the *Sx* and *Sm* facies, commonly ending with and *Sr* facies. Each cycle within this unit records the cutting and migration of an erosive-base fluvial channel (elements *CH*) that was subsequently infilled by lateral migration of point-bar deposits on inner channel bends (elements *LA* and *SB*). The arrangement of architectural elements within the Hualhuani Formation reflects the amalgamation of numerous sandy bars of braided-dominated environments. We interpret that these deposits are associated with the initiation of a braided fluvial system, in response to an increase in the topographic gradient of the alluvial plain more than a simple readjustment to the fall of the base level (see further discussions in the Section [8.3](#)). This interpretation highlights a drastic increase of sediment input into the basin, and suggest lateral and frontal progradation, as well as extensive avulsion with sediment migration and reduction of sinuosity (cf. [Miall, 2000](#)).

8. Discussions

The sedimentological evidences provided so far allow to obtain a consistent paleogeographic framework explaining the origin, transit and deposition of sediments along southern Peru, and also discuss the most critical points that would affect this model. Relative sea level fluctuations are also discussed here also in light of variable geodynamic conditions.

8.1. The definition of the sedimentary environments identified and their implications to paleogeography

[León \(1981\)](#), [Salinas \(1985\)](#), [Vicente et al. \(1982\)](#), [Vicente \(2005, 2006\)](#) and numerous later publications stated that in southern Peru, the facies of the Cachíos and Labra Formations correspond to turbidites of submarine fans of talus environments. Given the evidences for a high-sinuosity fluvial system (as stated in Section [7.1](#)), this study rejects any model including a submarine fan in Tacna. According to our

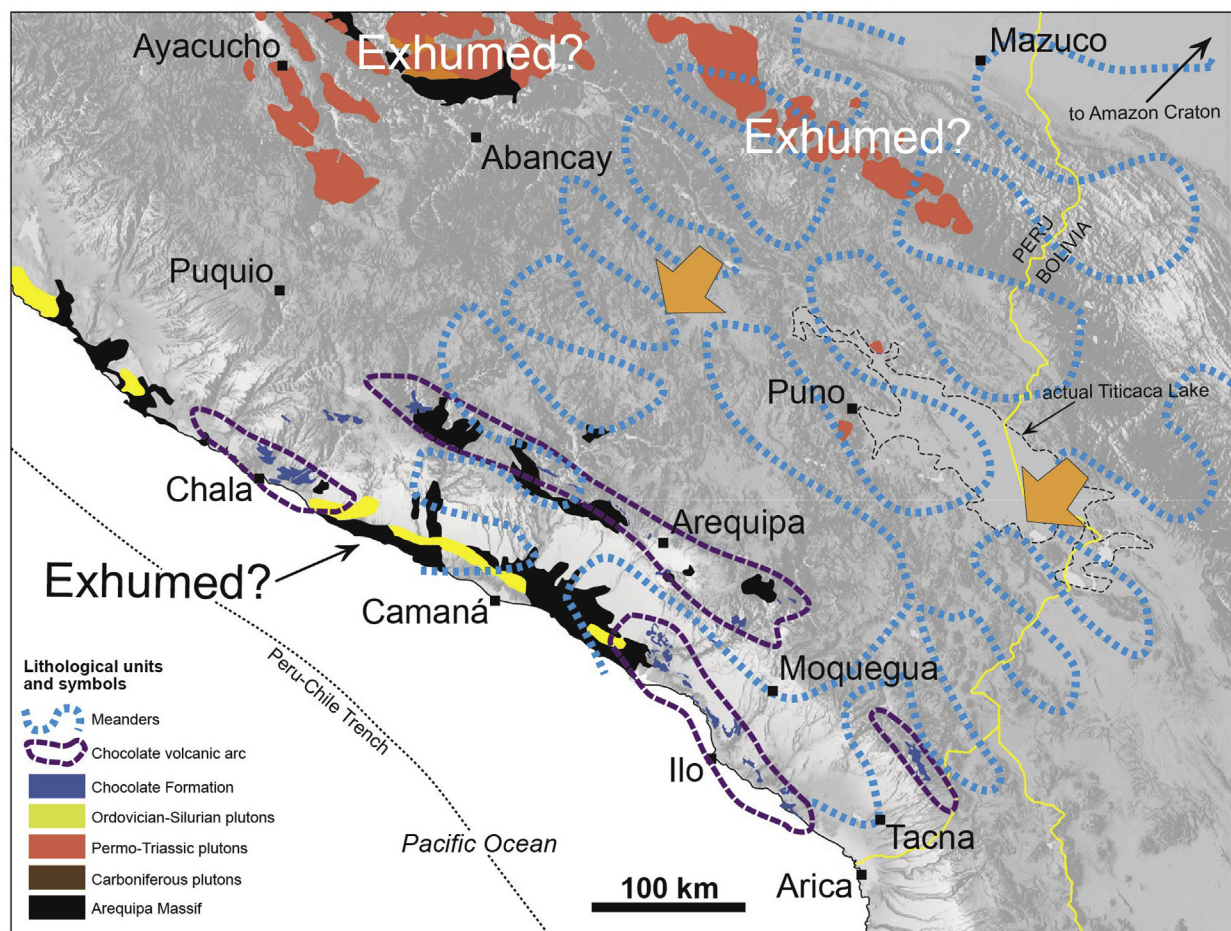


Fig. 15. Paleogeographic representation (not to scale) of the Arequipa-Tarapacá Basin in southern Peru and northern Chile during deposition of the Yura Group (Cachíos, Labra and/or Gramadal formations). The occurrence of the Chocolate Volcanic Arc is inserted in this graphic basing on the geological maps of INGEMMET (2016). The Chocolate Formation does not represent a significant positive relief for the compositional time studied. Pre-Mesozoic rocks compiled from Palacios et al. (1995) and Chew et al. (2008). Orange arrows indicate the preferential way of sediment transport. (For interpretation of the references to colour in this figure legend, the reader is referred to the web version of this article.)

interpretation, sediments of the Cachíos and Labra Formations of Tacna correspond to extensive fluvial meandering facies, with numerous point-bar and floodplain deposits (Fig. 15). Nonetheless, it is remarkable the occurrence of at least twice marine incursions, one during Callovian (within the Cachíos Formation) and another during some stage of the Tithonian age (within the Gramadal Formation). These evidences suggest two important points, (i) during the terrestrial deposition of the Yura Group, the paleo-Pacific Ocean was adjacent to the area of Tacna with topography being flat enough to allow extensive marine incursion represented by the presence of tidal (with ichnofacies similar to *Thalassinoides*, Fig. 8E) or even deltaic environments, and (ii) strong pulses of subsidence creating accommodation space and consequent large-scale marine incursion during Middle Callovian and some stage of the Tithonian (see Section 8.3 for further discussions).

Numerous slumps within the Cachíos Formation are documented in Arequipa, Moquegua as well as in Tacna (Fig. 6A and B, also cf. Vicente, 1981; Vicente et al., 1982; Sempere et al., 2002). According to Allen (1970), slumps occur at different scales and in a wide range of environments, including fluvial, deltaic and shallow marine environments. Therefore, the existence of slumps cannot be restricted to deep sea or talus environments as suggested by Vicente et al. (1982). Slumps occur when soft sediments are disturbed and reflect gravitationally unstable deposits (Allen, 1970). In southern Peru, slumps are more frequent in marine environments where Callovian ammonites are found. Marine incursions are not exclusive of the Cachíos Formation,

but are also documented in the Gramadal Formation. Because both marine incursions disrupt the typical signature of a fluvial system, suggest that such events might be consequence of local and/or regional tectonic activity (see Section 8.3 for further discussions).

Vicente (2006) stated that proximal facies of the Cachíos and Labra Formations are located northwest of Arequipa, while the distal facies would be those in Tacna, implying in this way a sediment transport to towards the south-east into northernmost Chile. Furthermore, the same author (Vicente, 2005) proposed that most of these sediments were derived from the erosion of the Chocolate Formation (Chocolate Volcanic Arc). We also reject the statement of the Chocolate Formation as main source of sediments for the Yura Group and the Hualhuani Formation. The compositional features described before support the conclusions of Wotzlaw et al. (2011) and a sediment routing system with very limited contributions from a western arc and identify the recycling of rocks conforming the eastern basin margin as the main source. We also identify a general transport of the sediments towards the southwest and/or west, but identify the recycling of the Amazon Craton and related sedimentary covers as the most probable area from which sediment were derived.

8.2. Stratigraphic reorganization of the Mesozoic rocks in Tacna

Sandy deposits of the Cachíos and Labra Formations display a gradually upward increase, reflecting the contemporaneous steady

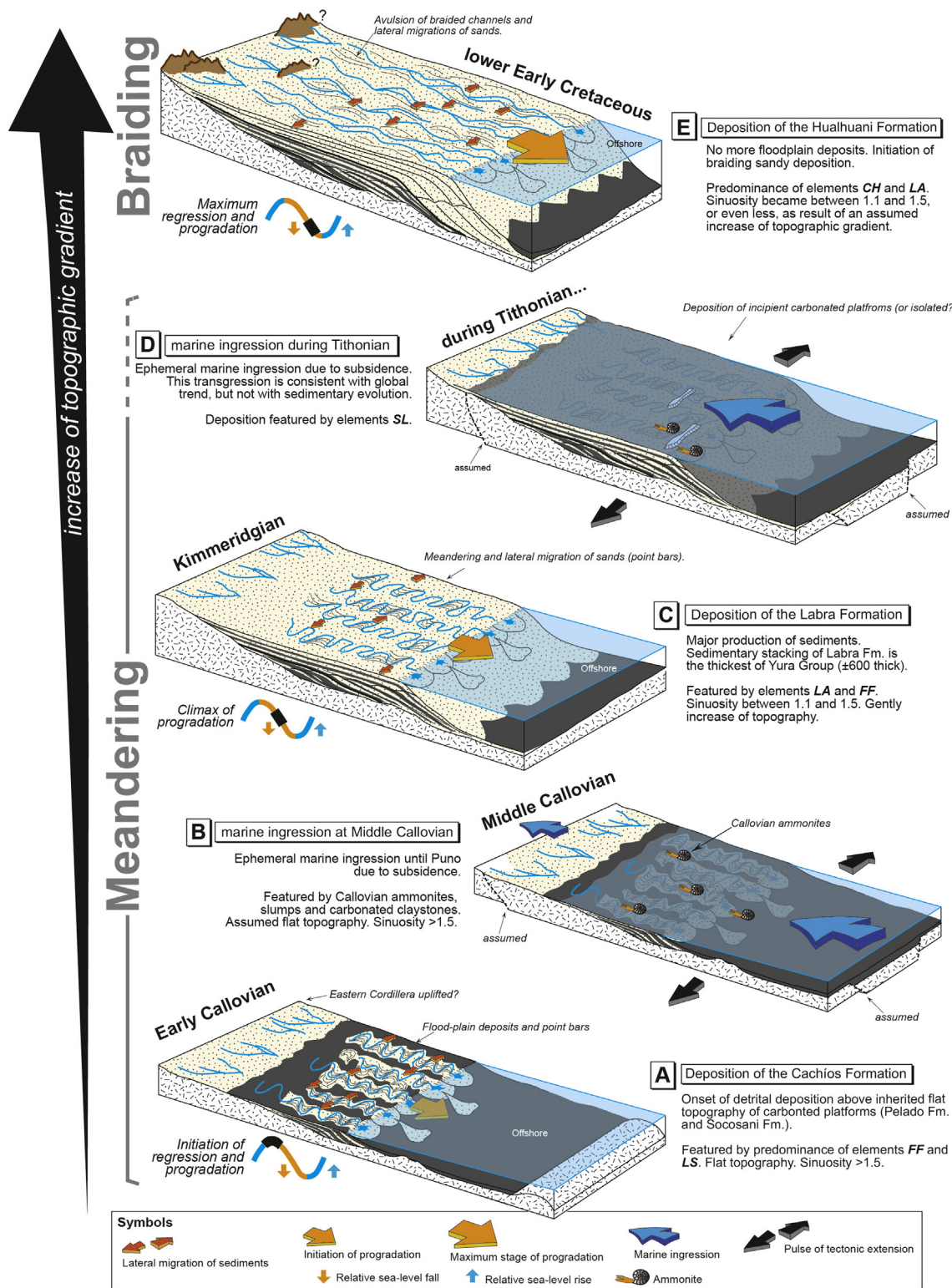


Fig. 16. Schematic diagrams of the sedimentary evolution and architecture of the Mesozoic sediments of Tacna (not to scale). In A: Initiation of meandering setting (Cachios Formation) reflecting high-sinuosity meanders flowing above an assumed semi-flat topography. In B: Schematic representation of a marine ingressions occurred during middle Callovian time. In C: Meandering setting of the Labra Formation (Kimmeridgian) reflecting increase of lateral accretion deposits. In D: Schematic representation of a marine ingressions occurred during Tithonian time. In E: Initiation of braiding depositional setting of the Hualhuani Formation (Early Cretaceous). This schema highlights at least two marine ingressions occurred during the deposition of Mesozoic sediments in Tacna (B and C).

reduction in sinuosity and increase of topographic gradient (see more detail in Section 8.3) making the identification of a well-defined stratigraphic boundary between the Cachios and Labra Formations (see proposal in the Fig. 11).

Furthermore, it is possible to mark a sharp boundary between the Hualhuani and Gramadal formations, and locally between the Hualhuani and Labra formations by using the marked erosional base within the depositional context of the CH architectural elements.

Besides this unconformity separates the two marked depositional settings (meanders vs. braided), we consider all these arguments enough to consider the Cachíos, Labra and Gramadal Formations as the only members of the Yura Group in Tacna. Moreover, we also propose the exclusion of the Hualhuani Formation from the Yura Group, which is therefore considered as an independent Early Cretaceous (Berriasian) lithostratigraphic unit. The Callovian facies of the Puente Formation s.s. Are not present in Tacna, but in Arequipa only. In Tacna, the Callovian facies correspond to the architectural elements *FF* of the Cachíos Formation.

The statement of a meandering fluvial system for the Cachíos and Labra Formations lead us to affirm that these units are widely extensive and highly correlatable for over 200 km width, as wide as any large present-day fluvial system of high sinuosity (e.g. Niger river, Miall, 2014). These elements are also helpful when performing stratigraphic correlations and other kind of basin analysis because of the architectural configuration of these units occurring without major variations in facies along southern Peru (e.g. Labra Formation).

8.3. Relative sea-level fluctuations versus geodynamics during Middle Jurassic to Early Cretaceous in Tacna

The Mesozoic sediments of Tacna (ca. 1300 m thick) represents a ca. 34 Ma cycle of fluvial progradation starting in the Callovian and ending around the early Lower Cretaceous (Fig. 16A). The deposition of the Mesozoic sediments shows a clear regressive nature, displaying both lateral and frontal westward and/or south-westward sediment migration. This depositional style contrasts with the correspondent global sea-level rise proposed by Haq et al. (1987) and Hardenbol et al. (1998) (Fig. 6). Progradation has therefore to be entirely related to local/regional tectonics, determining important phases of subsidence and creation of accommodation space. We highlight important modifications within the identified fluvial regressive evolution of Yura Group, which include at least two marine incursions identified from (i) Middle Callovian and (ii) Tithonian strata (Fig. 16B and D). Given the sudden marine incursions, which are accompanied to slumps and common volcanism (sills), we reinforce the corresponding episodes to stages of strong pulses of subsidence, typical of an extensional tectonic regime.

9. Conclusions

Four major conclusions are derived from the detailed sedimentologic and petrographic analysis carried out on the Mesozoic sediments of Tacna.

- (i) The nature of the detrital Mesozoic sediments of Tacna is fluvial (and eventual tidal influence), and have a strong progradational character throughout the time of deposition of ca. 34 Myr. Sedimentation initiated within a high-to moderate-sinuosity meandering setting since the Callovian until the Tithonian times followed by the onset of incipient braided setting since the lower Early Cretaceous (Berriasian). Sedimentary stacking patterns developed in response of a gently increase of the topographic gradient with the rifting of the Arequipa-Tarapacá Basin getting close to its end.
- (ii) Sediments deposited during the meandering phase are those of the Cachíos, Labra and Gramadal formations. During the Middle Callovian and some stages of the Tithonian strong pulses of subsidence and creation of accommodation space occurred and favoured the accumulation of marine carbonate sediments including ammonites accompanied by small volcanic activity. Sediments deposited during the braided phase are those of the Hualhuani Formation. The deposition of the Hualhuani Formation is featured by numerous channels with erosive bases, being the bottom of this unit the stratigraphic boundary with the underlying Gramadal Formation (and locally, directly with the Labra Formation).

- (iii) The Cachíos, Labra and Gramadal Formations conform the Yura Group of Tacna (Callovian to Tithonian), while the Hualhuani Formation (Berriasian) is excluded from this hierarchy. The Puente Formation s.s. is not exposed in Tacna.
- (iv) The Mesozoic sedimentary evolution in Tacna reflects the effects of a tectonically active (rift-type) basin over global eustasy. We argue that rifting involves subsidence (and consequent tilting and local/regional increase of topographic gradient) and subsidence of specific areas within the Arequipa Basin was rather active during sedimentary deposition. Such subsidence triggered periodical marine incursions. The marine incursions during the Middle Callovian and Tithonian times clearly suggest that marine influences occurred only at the cited stages, not during the whole evolution of the Yura Group and Hualhuani Formation.
- (v) Petrographic data revealed the composition of the Yura Group and the Hualhuani Formation which are mostly made of quartz-dominated sandstones (i.e. quartzarenite, subarkose and sublitharenite) and claystone. These deposits are derived predominantly from the recycling of sediments located to the east possibly corresponding to older sediments of the Amazon Craton. Contributions from the Jurassic volcanic arc is negligible as volcanic rock fragments, which are extremely rare and concentrated in the Cachíos, Labra and Gramadal formations only. This fact suggests that the potential limited arrivals from the Jurassic volcanic arc are restricted to the meandering phase and that modification of paleodrainages may have excluded it during the development of the braided phase.

Acknowledgements

The study was funded by Instituto Geológico Minero y Metalúrgico (INGEMMET) (POI GR41A 2015-2016, DGR) of Peru and co-funded by FONDECYT (CIENCIACTIVA of Peru) Convenio N° 216-2015 ("*Registro de variaciones climáticas en los sedimentos durante el Mesozoico y Cenozoico del Sur de Perú, 18°S*"). These results form part of the research project GR41A-2016 (INGEMMET) and the Sediment Research Workgroup (GeoSed, Peru). Field work, data interpretation and exhaustive discussions with Rildo Rodríguez, Harmuth Acosta, Alejandro Rosado, Cesar Chacaltana (Lima) and an anonymous reviewer strongly benefited this manuscript. We want to thanks to Astrid Criales for the support on the search of grants, as well as for her valuable advices on the manuscript organization and the graphic edition of an earlier version.

Appendix A. Supplementary data

Supplementary data related to this article can be found at <http://dx.doi.org/10.1016/j.jsames.2018.04.014>.

References

- Acosta, H., Alván, A., Mamani, M., Rodríguez, J., 2011. Geología de los Cuadrángulos de Pachía (36-v) y Palca (36-x). Escala 1:5,000. Serie A: carta Geológica Nacional. Dirección de Geología Regional, INGEMMET, Lima, Perú. Boletín 139, 96.
- Aldana, M., 1989. El Caloviano en la Hacienda Queirane, vol. 79. Departamento de Puno. Sociedad Geológica del Perú, Boletín, pp. 41–52.
- Allen, J.R.L., 1963. The classification of cross-stratified units with notes on their origin. *Sedimentology* 2, 93–114.
- Allen, J.R.L., 1970. Studies in fluvial sedimentation: a comparison of fining upwards cyclothem, with particular reference to coarse member composition and interpretation. *J. Sediment. Petrol.* 40, 298–323.
- Allen, 1982. Sedimentary structures: their character and physical basis. *Dev. Sedimentol.* 2, 1–593.
- Alván, A., 2009. Relación de las facies sedimentarias y de los ammonites del Jurásico inferior a medio (Arequipa) y Palquilla (Tacna). Tesis de Grado. Universidad Nacional Mayor de San Marcos, Perú, pp. 122.
- Alván, A., Vennari, V., Acosta, H., Borja, S., Giraldo, E., 2010. División y comparación Biozonal del Jurásico medio y superior en la Cuenca Arequipa, Sur de Perú: resultados Iniciales. In: XV Congreso Peruano de Geología, Cusco, Perú, Sociedad Geológica del Perú, Resúmenes Extendidos, 200–203.
- Bell, C.M., Suarez, M., 1995. Triassic alluvial braidplain and braided river deposits of the

- La Ternera Formation, Atacama region, northern Chile. *J. S. Am. Earth Sci.* 8 (1), 1–8.
- Bellido, E., Guevara, C., 1963. Geología de los Cuadrángulos de Punta de Bombón y Clemeles (Hojas 35-s y 35-t). Comisión Carta Geológica Nacional. Boletín 5, 92.
- Benavides, V., 1962. Estratigrafía Pre-terciaria de la región de Arequipa. In: Boletín de la Sociedad Geológica del Perú, II Congreso Nacional de Geología (Tomo 38), pp. 5–63.
- Benites, A., 2017. Variaciones del nivel del mar y cronozonas de amonites jurásicos en el sur de la Cuenca Arequipa (Sur de 17°S) Perú: Esquema evolutivo. Tesis de Bachiller. Universidad de Piura, Perú, pp. 177.
- Boekhout, F., Spikings, R., Sempere, T., Chiaradia, M., Ulianov, A., Schaltegger, U., 2012. Mesozoic arc magmatism along the southern Peruvian margin during Gondwana breakup and dispersal. *Lithos* 146–147, 48–64.
- Boekhout, F., Sempere, T., Spikings, R., Schaltegger, U., 2013. Late Paleozoic to Jurassic chronostratigraphy of coastal southern Peru: temporal evolution of sedimentation along an active margin. *J. S. Am. Earth Sci.* 47, 179–200.
- Caracciolo, L., Le Pera, E., Muto, F., Perri, F., 2009. Sandstone petrology and mudstone geochemistry of the peruc-korycany formation (bohemian cretaceous basin, Czech republic). *Int. Geol. Rev.* 1, 1–29.
- Carlotto, V., Rodríguez, R., Acosta, H., Cárdenas, J., Jaillard, E., 2009. Alto estructural Totos-Paras (Ayacucho): Límite paleogeográfico en la evolución mesozoica de las cuencas Pucará (Triásico superior-Liásico) y Arequipa (Jurásico-Cretácico). In: Boletín de la Sociedad Geológica del Perú, Volumen Especial N° 7: Victor Benavides Cáceres, p. 1–46.
- Chew, D.M., Magna, T., Kirkland, C.L., Miskovic, A., Cardona, A., Spikings, R., Schaltegger, U., 2008. Detrital zircon fingerprint of the Proto-Andes: evidence for a Neoproterozoic active margin? *Precambrian Res.* 167, 186–200.
- Clark, A., Farrar, E., Woodman, P., Wastnneys, H., Sandeman, H., Archibald, D., 1990. Geologic and geochronologic constraints on the metallogenic evolution of the Andes of southeastern Peru. *Econ. Geol.* 85, 1520–1583.
- Davis, R.A., 2012. Chapter 3: tidal signatures and their preservation potential in stratigraphic sequences. In: Davis, R.A., Dalrymple, R.W. (Eds.), *Principles of Tidal Sedimentology*. Springer Science & Business Media, pp. 35–77.
- Dickinson, W.R., Suczek, C.A., 1979. Plate tectonics and sandstone compositions. *Am. Assoc. Petrol. Geol.* 63 (12), 2164–2182.
- Dickinson, W.R., Lawton, T.F., Inman, K.F., 1985. Sandstone detrital modes, central Utah foreland region: stratigraphic record of Cretaceous-Paleogene tectonic evolution. *J. Sediment. Petrol.* 56 (2), 276–293.
- Dunham, R.J., 1962. Classification of carbonate rocks according to depositional texture. In: Ham, W.E. (Ed.), *Classification of Carbonate Rocks*. American Association of Petroleum Geologists, Memoir 1, pp. 108–121.
- Embry, A.F., Klovan, J.E., 1971. A late devonian reef tract on northeastern banks island. *NWT. Canadian Petrol. Geol. Bulletin* 19, 730–781.
- Fielding, C.R., Webb, J.A., 1996. Facies and cyclicity of the late permian bainmedart coal measures in the northern prince charles mountains, MacRobertson land, Antarctica. *Sedimentology* 43, 295–322.
- Freytet, P., Plaziat, J.C., 1982. Continental carbonate sedimentation and pedogenesis-Late Cretaceous and Early Tertiary of southern France. *Contrib. Sedimentol.* 12 1.213.
- Hag, B., Hardenbol, J., Vail, P., 1987. Chronology of fluctuating sea levels since the triassic (250 million years ago to present). *Science* 235, 1156–1167.
- Hardenbol, J., Thierry, J., Farley, M., Jacquin, T., De Graciansky, P.C., Vail, P., 1998. Mesozoic and cenozoic sequence stratigraphy of europeans basins, mesozoic and cenozoic sequence chronostratigraphic framework of europeans basins. *SEPM (Soc. Sediment. Geol.) Spec. Publ.* 60, 3–13.
- Hughes, Z.J., 2012. Chapter 11: tidal channels on tidal flats and marshes. In: Davis, R.A., Dalrymple, R.W. (Eds.), *Principles of Tidal Sedimentology*. Springer Science & Business Media, pp. 269–299.
- INGEMMET, 2016. Informe sedimentológico y lito-bioestratigráfico del Proyecto GR41A (Geología de la Cuenca Sedimentaria Peruana Occidental entre 15° y 18°S) de la Dirección de Geología Regional. Reporte Interno. pp. 89.
- Ingersoll, R.V., Bullard, T.F., Ford, R.L., Grimm, J.P., Pickle, J.D., Sares, S.W., 1984. The effect of grain size on detrital modes: a test of the Gazzi-Dickinson point-counting method. *J. Sediment. Res.* 54 (1), 103–116.
- Jaillard, E., Jacay, J., 1989. Les "Couches Chicama" du Nord du Perou: colmatage d'un bassin né d'une collision oblique au thionique. *C.R. Acad. Sci. Paris* 308 (II), 1459–1465.
- Jaillard, E., Soler, P., Carlier, G., Mourier, T., 1990. Geodynamic evolution of the northern and central Andes during early to middle Mesozoic times: a Tethyan model. *J. Geol. Soc.* 147, 1009–1022.
- Jaillard, E., Herail, G., Monfret, T., Díaz-Martínez, E., Baby, P., Lavenue, A., Dumont, J.F., 2000. Tectonic evolution of the Andes of Ecuador, Peru, Bolivia and northernmost Chile. In: Cordani, U., Milani, E.J., Thomaz, A., Campos, D.A. (Eds.), *Tectonic Evolution of South America*. Rio de Janeiro, Brazil, pp. 481–559.
- Jenks, W.F., 1945. La geología de Arequipa y sus alrededores. Informaciones y Memorias Sociedad de Ingenieros del Perú 46 (9), 1–104.
- León, I., 1981. Antecedentes sedimentológicos sobre el Jurásico-Cretácico inferior del sector de Yura (Departamento de Arequipa). PhD thesis. Universidad Nacional San Agustín, Perú, pp. 92.
- Mamani, M., Wörner, G., Sempere, T., 2010. Geochemical variations in igneous rocks of the Central Andean orocline (13°S to 18°S): tracing crustal thickening and magma generation through time and space. *Geol. Soc. Am.* 122, 162–182.
- Martínez, W., Cervantes, J., 2003. Rocas ígneas en el Sur del Perú. Nuevos Datos Geocronológicos, Geoquímicos y Estructurales entre los paralelos 16° y 18°30' Latitud Sur. Serie D: estudios Regionales, Dirección de Geología Regional, INGEMMET. Boletín 26, 146.
- Martínez, F., Arriagada, C., Mpodozis, C., Pena, M., 2012. The Lautaro Basin: a record of inversion tectonics in northern Chile. *Andean Geol.* 39 (2), 258–278.
- McBride, E.F., 1963. A classification of common sandstones. *J. Sediment. Petrol.* 33 (3), 664–669.
- Miall, A.D., 1985. Architectural-element analysis: a new method of facies analysis applied to fluvial deposits. *Earth Sci. Rev.* 22, 261–308.
- Miall, A.D., 1996. *The Geology of Fluvial Deposits: Sedimentary Facies, Basin Analysis, and Petroleum Geology*. Springer-Verlag, New York, pp. 582.
- Miall, A.D., 2000. *Principles of Sedimentary Basin Analysis*. 3rd, updated and enlarged version. Springer, pp. 616.
- Miall, A.D., 2014. *Fluvial Depositional Systems*. Springer-Cham, Berlin, pp. 322.
- Monge, R., Cervantes, J., 2000. Memoria explicativa de la Geología del Cuadrángulo de Pachía y Palca (36-v). INGEMMET, Lima, Perú, pp. 11.
- Nanson, G.C., Croke, J.C., 1992. A genetic classification of floodplains. *Geomorphology* 1 (6), 159–186.
- Ochoa, M., Arribas, J., Mas, R., Goldstein, R.H., 2007. Destruction of a fluvial reservoir by hydrothermal activity (Camerós basin, Spain). *Sediment. Geol.* 202, 158–173.
- Oliveros, V., Féraud, G., Aguirre, L., Fornari, M., Morata, D., 2006. The early andean magmatic province (eamp): ⁴⁰Ar/³⁹Ar dating on mesozoic volcanic and plutonic rocks from the coastal cordillera, northern Chile. *J. Volcanol. Geoth. Res.* 157, 311–330.
- Oliveros, V., Labbé, M., Rossel, M., Charrier, R., Encinas, A., 2012. Late Jurassic paleogeographic evolution of the Andean back-arc basin: new constraints from the Lagunillas Formation, northern Chile (27°30'–28°30'). *J. S. Am. Earth Sci.* 37, 25–40.
- Oncken, O., Hindle, D., Kley, J., Elger, K., Victor, P., Schemmann, K., 2006. Chapter 1: deformation of the Central Andean Upper Plate system-facts, fiction, and constraints for the plateau models. In: Oncken, O., Chong, G., Franz, G., Giese, P., Götze, H.J., Ramos, V.A., Strecker, M.R., Wigger, P. (Eds.), *The Andes, Active Subduction Orogeny*, pp. 1–27.
- Palacios, O., 1995. Geología del Perú. INGEMMET, Lima, Perú. Boletín N° 55, Serie A: Carta Geológica Nacional. pp. 143.
- Palacios, O., Sánchez, A., Herrera, F., 1995. Geología del Perú. INGEMMET, Dirección de Geología Regional, Perú. Boletín No. 55, Serie A: Carta Geológica Nacional. pp. 198.
- Parent, H., 2006. Oxfordian and late callovian ammonite faunas and biostratigraphy of the neuquén-mendoza and tarapacá basins (jurassic, ammonoidea, western south America). *Bol. del Inst. Fisiogr. Geol.* 76 (1), 1–70.
- Plint, A.G., 1983. Sandy fluvial point bar sediments from the middle eocene of dorset, england. In: Collinson, J.D., Lewin, J. (Eds.), *Modern and Ancient Fluvial System: International Association of Sedimentologists*. vol. 6. Special Publications, pp. 355–368.
- Quispe, Y., 2016. Facies y geoquímica de rocas carbonatadas del Jurásico inferior-medio de la Cuenca de Arequipa en el Departamento de Tacna: Paleogeografía y Geodinámica. Tesis de Bachiller. Universidad Nacional del Altiplano, Perú, pp. 126.
- Ramos, V.A., 2009. The tectonic regime along the Andes: present-day and Mesozoic regimes. *Geol. J.* 45, 2–25.
- Ramos, V.A., Aleman, A., 2000. Tectonic evolution of the Andes. In: Cordani, U.G., Milani, E.J., Thomaz, A., Campos, D.A. (Eds.), *Tectonic Evolution of South America*, Rio de Janeiro, Brazil, pp. 635–685.
- Roberts, E.M., 2007. Facies architecture and depositional environments of the upper cretaceous kaiparowits formation, southern Utah. *Sediment. Geol.* 197, 207–233.
- Salinas, E., 1985. Evolución paleogeográfica del Sur del Perú a la luz de los métodos de análisis sedimentológicos del departamento de Tacna. Arequipa, Perú. Tesis de Maestría. Universidad Nacional San Agustín de Arequipa, Perú, pp. 205.
- Schumm, S.A., 1981. Evolution and Response of the Fluvial System, Sedimentologic Implications. *The Society of Economic Paleontologists and Mineralogists (SEPM)*, pp. 19–29 Special Publications N° 31.
- Sempere, T., Carlier, G., Soler, P., Fornari, M., Carlotto, V., Jacay, J., Arispe, O., Néraudeau, D., Cárdenas, J., Rosas, S., Jiménez, N., 2002. Late permian–middle jurassic lithospheric thinning in Peru and Bolivia, and its bearing on andean-age tectonics. *Tectonophysics* 345, 153–181.
- Smith, N.D., Cross, T.A., Dufficy, J.P., Clough, S.R., 1989. Anatomy of an avulsion. *Sedimentology* 36, 1–23.
- Stehn, E., 1923. Beiträge zur Kenntnis des Bathonien und Callovien in Südamerika. *Neues Jahrbuch für Mineralogie, Geologie und Palaeontologie, Beilage/Band N° 49*. pp. 52–158.
- Trinidad, I., 2017. Procedencia sedimentaria de la Cuenca mesoica Arequipa en Tacna (18°S) a traves de los minerales pesados. Tesis de Ingeniero Geólogo. Universidad Nacional Daniel Alcides Carrión, Perú, pp. 120.
- Vail, P.R., Audemard, E., Bowman, S.A., Eisner, P.N., Perez-Cruz, C., 1991. The stratigraphic signatures of tectonics, eustasy and sedimentology-an overview. In: Einsele, G., Ricken, W., Seilacher, A. (Eds.), *Cycles and Events in Stratigraphy*, pp. 617–659. Springer-Verlag, Berlin, pp. 955.
- Vargas, L., 1970. Geología del Cuadrángulo de Arequipa. INGEMMET, Lima, Perú. Boletín No. 24, Serie A: Carta Geológica Nacional. pp. 64.
- Vicente, J.C., 1981. Elementos de la estratigrafía Mesozoica sur Peruana. Comité Sudamericano del Jurásico y Cretácico. In: Volkheimer, I., Musacchio, A. (Eds.), *Cuencas sedimentarias del jurásico y cretácico de America del sur*. vol. 1. pp. 319–351.
- Vicente, J.C., 1989. Early late Cretaceous overthrusting in the western cordillera of southern Peru. In: Ericksen, G.E., Canas Pinochet, M.T., Reinemund, J.A. (Eds.), *Geology of the Andes and its Relation to Hydrocarbon and Mineral Resources*, vol. 11. Circum-Pacific Council for Energy and Mineral Resources Earth Science Series, Houston, Texas, pp. 91–117.
- Vicente, J.C., 2005. Dynamic paleogeography of the Jurassic Andean basin: pattern of transgression and localization of main straits through the magmatic arc. *Rev. Asoc. Geol. Argent.* 60, 221–250.
- Vicente, J.C., 2006. Dynamic paleogeography of the Jurassic Andean basin: pattern of regression and general considerations on main features. *Rev. Asoc. Geol. Argent.* 61, 408–437.

- Vicente, J.C., Beaudoin, B., Chávez, A., León, T., 1982. La cuenca de Arequipa (Sur Perú) durante el Jurásico y Cretácico Inferior. V Congreso Latinoamericano de Geología 1, 121–153.
- Víseras, C., Fernández, J., 2010. Capítulo 8: Sistemas aluviales de alta sinuosidad. In: Arche, A. (Ed.), *Sedimentología: Del Proceso Físico a la Cuenca Sedimentaria*. Consejo Superior de Investigaciones Científicas, pp. 1290.
- von Hillebrandt, A., 1987. Liassic Ammonite Zones of South America and Correlations with Other Provinces. *Circum-Pacific Jurassic Contribution to I.G.C.P. # 171*. pp. 111–157.
- von Hillebrandt, A., Schmidt-Effing, R., 1981. Ammoniten aus dem Toarcium (Jura) von Chile (Sudamerika). *Zitteliana* 6, 3–74.
- Westermann, G.E.G., 1996. In: Landman, N.H., Tanabe, K., Davis, R.A. (Eds.), *Ammonoid Life and Habitat. Ammonoid Paleobiology*. vol. 13. Plenum Press, New York, pp. 607–707.
- Westermann, G.E.G., Riccardi, A., Palacios, O., Rangel, C., 1980. Jurásico Medio en el Perú. Serie D: estudios Regionales. Dirección de Geología Regional, INGEMMET, Lima, Peru. Boletín 9, 63.
- Wilson, J., García, W., 1962. Geología de los Cuadrángulos de Pachá y Palca (Hojas 36-v y 36-x). Dirección de Geología Regional, INGEMMET, Lima, Perú. Boletín N° 4, Serie A: Comisión de la Carta Geológica Nacional. pp. 82.
- Wotzlaw, J.F., Decou, A., von Eynatten, H., Wörner, G., Frei, D., 2011. Jurassic to Paleogene tectono-magmatic evolution of northern Chile and adjacent Bolivia from detrital zircon U-Pb geochronology and heavy mineral provenance. *Terra. Nova* 23, 399–406.
- Zuffa, G.G., 1980. Hybrid arenites: their composition and classification. *J. Sediment. Petrol.* 50 (1), 21–29.